I. PROPERTIES OF RAT LIVER CYTOPLASMIC GLUCOSE 6-PHOSPHATE DEHYDROGENASE

II. IMPROVEMENTS IN NUMERICAL METHODS FOR ANALYZING PROTON AND METAL-LIGAND EQUILIBRIUM CONSTANTS, AND APPLICATION TO THE MAGNESIUM: 5-PHOSPHORIBOSYL-1-PYROPHOSPHATE SYSTEM

By

RICHARD EDWARD THOMPSON

Bachelor of Science
Wichita State University
Wichita, Kansas
1968

Master of Science
Wichita State University
Wichita, Kansas
1969

Submitted to the Faculty of the Graduate College
of the Oklahoma State University
in partial fulfillment of the requirements
for the Degree of
DOCTOR OF PHILOSOPHY
May, 1974

I. PROPERTIES OF RAT LIVER CYTOPLASMIC GLUCOSE 6-PHOSPHATE DEHYDROGENASE

II. IMPROVEMENTS IN NUMERICAL METHODS FOR ANALYZING PROTON AND METAL-LIGAND EQUILIBRIUM CONSTANTS, AND APPLICATION TO THE MAGNESIUM: 5-PHOSPHORIBOSYL-1-PYROPHOSPHATE SYSTEM

Thesis Approved:

H. Thomas Tenney
Thesis Adviser

E. J. Eisenbraun

Robert K. Gholson

Roger E. Koeppe

J. P. Chandler

N. M. Durham
Dean of the Graduate College

ACKNOWLEDGEMENTS

The author would like to extend appreciation to his research adviser, Dr. H. O. Spivey, for advice, guidance, and support throughout the completion of work for this thesis. Appreciation is also extended Dr. J. P. Chandler of the Computer Science Department for the many hours spent helping the author with the numerical analysis involved in the thesis. In addition gratitude is extended Drs. R. E. Koeppe, R. K. Gholson, and E. J. Eisenbraun as Advisory Committee Members, and to the biochemistry faculty. The author extends special appreciation to Mr. Alan J. Katz for his thoughtful and meticulous help on the PRPP project.

The author wishes to express his appreciation to his wife for her encouragement and patient understanding throughout the duration of this study.

Thanks is also extended the Oklahoma State University Biochemistry Department for financial support.

TABLE OF CONTENTS

TABLE OF CONTENTS (Continued)

LIST OF TABLES

LIST OF FIGURES

Figure Page

PART ONE

PART TWO

LIST OF SYMBOLS AND ABBREVIATIONS

Σ = Greek capital sigma, indicating summation.

λ = Greek lambda.

χ = Greek chi.

θ = Greek theta.

μ = Greek micron.

G6PDH = Glucose 6-phosphate dehydrogenase.

LDH = Lactate dehydrogenase.

PEP = Phosphoenolpyruvate.

DHGA = Dehydroepiandrosterone.

G6P = Glucose 6-Phosphate.

PRPP = 5-Phosphoribosyl-1-pyrophosphate.

PART ONE

PROPERTIES OF RAT LIVER CYTOPLASMIC GLUCOSE 6-PHOSPHATE DEHYDROGENASE

CHAPTER I

INTRODUCTION

The pentose phosphate pathway occurs widely in living cells. The primary functions of the pathway are the production of pentose phosphate for nucleotide biosynthesis and the reduction of $NADP^+$ to NADPH for use in lipid biosynthesis and other specific reductions. It is through NADPH production by the first and third enzymes in the pathway that carbohydrate oxidation and lipid biosynthesis are related. The reaction catalyzed by glucose 6-phosphate dehydrogenase (G6PDH, D-glucose 6-phosphate:$NADP^+$ oxidoreductase, EC1.1.1.49) is markedly displaced from equilibrium in rat liver cells (1). These facts together with the key position of G6PDH at a metabolic branch point suggest that the G6PDH reaction may well be an important site for metabolic control. This view is supported by the fact that G6PDH shares several structural and functional properties with other regulatory enzymes. These include fluctuations in activity as a function of a variety of hormonal and nutritional states (2,3), its quaternary structure, and various effectors including fatty acids (4).

The cytoplasmic G6PDH of mammalian liver has been purified to apparent homogeniety in a number of laboratories (5-7). Its quaternary structure has resulted in somewhat contradictory conclusions from the several laboratories which have investigated the dissociation of the enzyme (6,8,9). The state of aggregation appears to be a function of enzyme

concentration (4). This is supported by studies on the enzyme from human erthrocytes which have demonstrated that the specific activity varies from 175 at an enzyme concentration of 0.3 mg/ml to 750 at 2 mg/ml. (10) The kinetic properties of liver G6PDH as a function of enzyme concentration have not been previously investigated.

The steady state kinetic mechanism of glucose 6-phosphate dehydrogenase has been studied using enzymes from Candida utilis (11), human erythrocyte (12), and Leuconostoc mesenteroides (13). Enzyme from these sources represent each of the three classes into which G6PDH may be divided on the basis of nucleotide specificity (13). The enzyme from C. utilis catalyzes only the NADP-dependent oxidation of G6P. Data based on initial velocity and NADPH product inhibition studies are consistent with a simple, ordered, sequential mechanism in which $NADP^+$ is bound first and NADPH released last (11). This is true also of the NADP-linked reaction catalyzed by G6PDH from L. mesenteroides (13), however, kinetic studies on this enzyme of the NAD-linked reaction indicated a more complex mechanism which requires an isomerization of free enzyme. Data collected on G6PDH from human erythrocytes indicate that it too follows an ordered, sequential mechanism with nucleotide adding first and being released last from the enzyme. The situation with G6PDH from erythrocyte as well as from C. utilis is further complicated by the existence of sigmoid kinetics when $[NADP^+]$ is varied. This has been extensively studied using erythrocyte enzyme (14,15). Studies on the steady state mechanism of G6PDH from all sources are limited by the inability to characterize the reverse reaction due to the marked instability of δ-gluconolactone 6-phosphate which has a half-life of 1.5 minutes in aqueous solutions at pH 7.4 (16).

CHAPTER II

STEADY STATE KINETIC PROPERTIES

Introduction

Previous steady state kinetic studies on rat liver cytoplasmic, G6PDH concerned themselves with the effect of substitiation at C-2 of G6P on the reaction rate (17), nucleotide specificity (18,19), and substrate and product inhibition (19). While the enzyme has been purified to near homogeniety by disc-gel electrophoresis and ultracentrifugation criteria in several laboratories to specific activities of 172 (20), 142 (5), 134 (7), and 210 (6), the previous steady state kinetic measurements have been done on enzyme with a specific activity of less than 0.5 U/ml. Since at least one property, nucleotide specificity, of the enzyme has been shown to vary as a function of purity (19) and in light of evidence that three different G6PDH-inactivating proteins exist in rat liver cells (21), it was deemed appropriate to attempt an elucidation of the steady state kinetic mechanism on purified enzyme.

Materials and Experimental Procedures

Glucose 6-phosphate, tetrasoidum NADP, NADPH, glucosamine 6-phosphate, and yeast glucose 6-phosphate dehydrogenase were purchased from Sigma. Glucose 6-phosphate (G6P) and $NADP^+$ were assayed using either rat liver or yeast G6PDH in 100 mM Tris-HCl, pH 8.0, containing 4.0 mM

$MgCl_2$ (assay buffer). The reaction rate measurements were made in a Coleman 124 spectrophotometer with a thermostated cell holder kept at 25 ± 0.1°C. All pH measurements were made on a Fisher model 320 pH meter at room temperature. Protein concentration was determined by the method of Lowry (22) with bovine serum albumin (Pentex) as a standard. The high carbohydrate, low fat rat diet was supplied by Nutritional Biochemicals Company.

Enzyme Purification

The enzyme was purified according to Holton's (6) modifications of the method by Matsuda and Yugari (7) with minor alterations. Holtzman strain albino rats were fasted two days and fed a high carbohydrate, low fat diet for three days prior to sacrifice. The liver was homogenized in a Waring blender. The CM-cellulose (Reeve-Angel) column was eluted with a linear gradient of 600 ml 20 mM NH_4Ac, pH 5.5 and 600 ml 50 mM potassium phosphate, pH 7.0 each containing 10^{-4}M $NADP^+$. All buffers used contained 5 mM β-mercapto ethanol and 0.1 mM EDTA. The enzyme was concentrated in diaflow ultrafiltration membranes (Schleicher and Scuell). All enzyme storage buffers contained 0.1 mM $NADP^+$.

Data Analysis

Data which conformed to a sequential initial velocity pattern were fitted to Equation (2-1)

$$v = \frac{V A B}{K_{ia} K_b + K_a B + K_b A + AB} \qquad (2\text{-}1)$$

where A and B represent $NADP^+$ and G6P concentrations respectively, V is

the maximum velocity, K_a and K_b represent the Michaelis constants for $NADP^+$ and G6P respectively, and K_{ia} is the $NADP^+$ dissociation constant. Curve fitting to this and each subsequent equation was done by the FORTRAN program package VINIT written in this laboratory which utilizes the optimization subroutine STEPIT (23) to minimize a sum of squares F defined by Equation (2-2).

$$F = \sum_{i=1}^{N} \left\{ \frac{Y_{i,exp} - Y_{i,calc}}{\sigma_i} \right\}^2 \qquad (2\text{-}2)$$

where $Y_{i,exp}$ is the measured velocity, $Y_{i,calc}$ is the computed velocity, σ_i is the standard error in the measured velocity, taken to be 5% of the measured velocity from repeated measurements, and N is the number of data points. The VINIT package is advantageous over similar programs in that any parameter(s) may be fixed at values determined from previous experiments designed specifically for the accurate determination of those parameters. This avoids the problem of an inaccurately fixed parameter assuming some physically unrealistic value in order to give an arbitrarily good fit. The program prints out the fitted parameter values, errors in these values based on the usual linear approximation (24), the correlations among the parameters, and an estimate of the quality of the fit in that the function F at the minimum is equivalent to the chi-square criterion for goodness-of-fit (25).

For product inhibition studies Equation (2-3) was used.

$$v = \frac{V A B}{K_{ia} K_b + K_b A + K_a B + AB + \frac{Q}{K_{iq}} (K_{ia} K_b + K_a B)} \qquad (2\text{-}3)$$

where K_{ia}, K_b, K_a, A, B, and V are as defined above, Q is the NADPH concentration, and K_{iq} is an inhibition constant (26). For dead-end inhibi-

tor studies using glucose or glucosamine 6-P, glucose 6-P analogs, Equation (2-4) was used.

$$v = \frac{V A B}{K_{ia} K_b + K_a B + K_b A (1 + \frac{I}{K_i}) + AB} \quad (2\text{-}4)$$

where I is the inhibitor concentration and K_i is the dissociation constant of I from the EAI complex. For inhibition studies in which both a dead-end inhibitor and a product were present Equation (2-5) was used.

$$v = \frac{V A B}{K_{ia} K_b + K_a B + K_b A (1 + \frac{I}{K_i}) + AB + \frac{Q}{K_{iq}} (K_{ia} K_b + K_a B)} \quad (2\text{-}5)$$

Results and Discussion

Initial Velocity Kinetics

Preliminary measurements for which G6P and $NADP^+$ concentrations were varied indicated that the K_m for $NADP^+$ was 1-5 μM. This is in agreement with 1.1 μM previously reported (19). For an accurate determination of this parameter it is necessary to measure initial velocities at substrate concentrations in the range of the K_m. However, in a standard 1 cm pathlength assay cuvette with an $NADP^+$ concentration of 1.0 μM, the net ΔA for the complete reaction is 0.012. Considering the initial velocity region of the reaction to be linear for the first 10% of the reaction this necessitates measuring velocity over a change of approximately 1 milliabsorbance unit. Therefore, initial velocity measurements for the determination of the K_m for $NADP^+$ were done in a 10 cm pathlength quartz cuvette. Figure 1 illustrates the experimental data and fitted curves. Table I (Fit 1) shows the results of the fit to Equation (2-1).

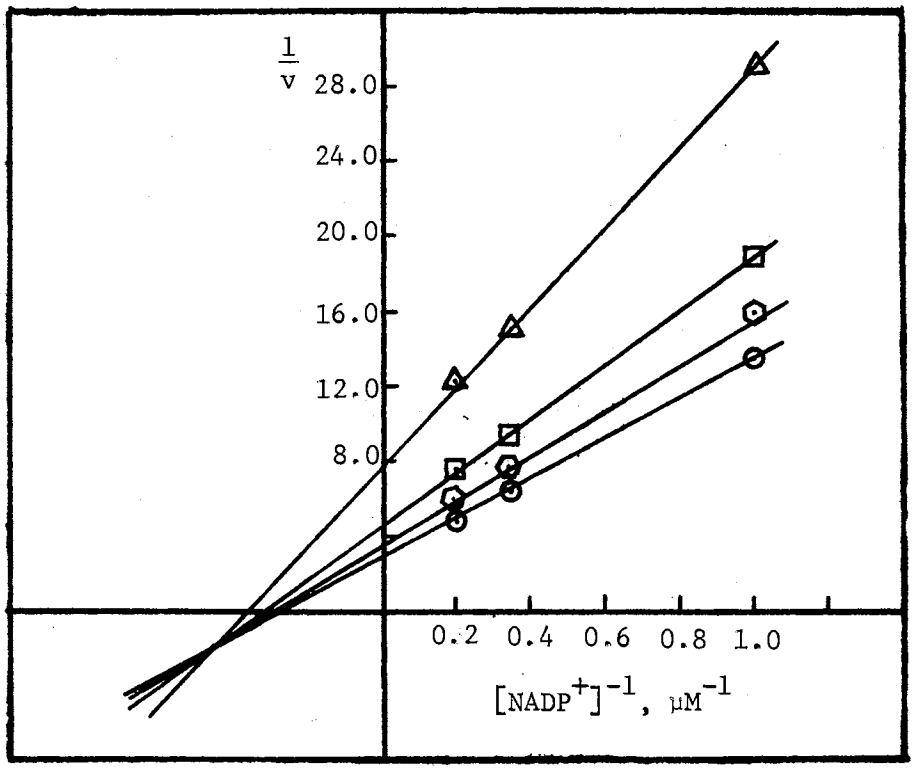

Figure 1. Initial Velocity Pattern of G6PDH. Measurements were performed at 25°C in 100 mM, pH 8.0 Tris, 4.0 mM $MgCl_2$. G6P concentrations were 20 µM, Δ-Δ, 50 µM, □ - □ ; 100 µM, ⬡ - ⬡ ; and 200 µM, O-O.

TABLE I

RESULTS OF REGRESSION ANALYSIS OF INITIAL VELOCITY DATA

Parameter	Fit 1	Fit 2
K_{NADP}	3.79 ± 0.40 μM	Fixed
K_{G6P}	40.9 ± 6.1 μM	51.2 ± 5.5 μM
K_{ia}	2.30 ± 0.48 μM	Fixed
χ^2	15.5	23.7
D.F.[b]	20	30

[a]Dissociation constant for the enzyme-NADP complex.

[b]Degrees of freedom.

Fit 2 of Table I is the result of fitting Equation (2-1) to initial velocity data collected at higher $NADP^+$ concentrations in a 1 cm pathlength cuvet system. For this fit the parameters K_a and K_{ia} were constrained to the fitted values from Fit 1 and K_b and V were allowed to vary. The quality of this fit as evidenced by the chi-square criterion ($\chi^2 = 23.7$) (a chi-square approximately equal to the number of degrees of freedom is expected) as well as the fitted value for K_b of 51 μM within experimental error of the fitted value of 40.9 μM from Fit 1 attest the validity of a comparison between the separate experiments. These results are in fair agreement with those previously reported (19) particularly in the values for K_b. However, the difference in K_a values is due probably to the inability of earlier workers to adequately measure velocities at low $NADP^+$ concentrations. One additional laboratory (17) has published steady-state kinetic results for the liver enzyme listing fitted values for the parameters. Although the data were analyzed using the sequential model (Equation 2-1) the authors assumed G6P to be the first and $NADP^+$ the second substrate to add to the enzyme. In addition the enzyme used was of particularly low specific activity (< 0.5 unit/mg). Therefore the reported values for K_{NADP+} of 15 ± 5 μM and K_{G6P} of 70 ± 17 μM from that laboratory are suspect.

Product Inhibition Studies

That product inhibition patterns are capable of demonstrating the order of addition of substrates in a sequential Bi-Bi mechanism has been well established (27). Previous workers have found NADPH to be linear competitive with respect to $NADP^+$ and linear noncompetitive with respect to G6P in erythrocyte (42), C. utilis (14), and L. mesenteroides (13).

This is in contrast to work on rat muscle G6PDH (19) which shows NADPH to competitively inhibit with respect to both $NADP^+$ and G6P. Figure 2 shows the result of fitting Equation (2-3) to data collected in an experiment in which the $NADP^+$ concentration was varied at several NADPH concentrations. The parameters K_a, K_{ia}, and K_b were held fixed at previously determined values (Fit 1) and K_{iq} was determined to be 15.9 ± 0.6 μM. Chi-square was 26.5 with 38 degrees of freedom indicating a satisfactory fit. The inhibition pattern is linearly competitive. Figure 3 shows a plot of results obtained from an experiment in which G6P was the variable substrate and NADPH the product inhibitor. The solid lines are the result of fitting to Equation (2-3) and indicate a linear non-competitive product inhibition pattern. The fitted value for K_{iq} was 11.0 ± 2.1 μM in good agreement with the fitted value determined with $NADP^+$ as variable substrate. Chi-square for the fit was 19.2 (36 degrees of freedom).

Product inhibition studies using 6-Phospho-δ-gluconolactone are impractical due to the instability of the compound in aqueous solution (16).

Dead-End Inhibition Studies

In 1964 Fromm (28) showed how competitive inhibitors might be used to distinguish between ordered and random mechanisms for two substrate enzymes. A second advantage of using compounds which compete with a substrate for the same enzymic site in ordered systems is that the order of substrate addition can be determined. It has been shown that glucosamine 6-P is a competitive inhibitor with respect to G6P in the G6PDH catalyzed reaction (17). For this reason glucosamine 6-P was used as a

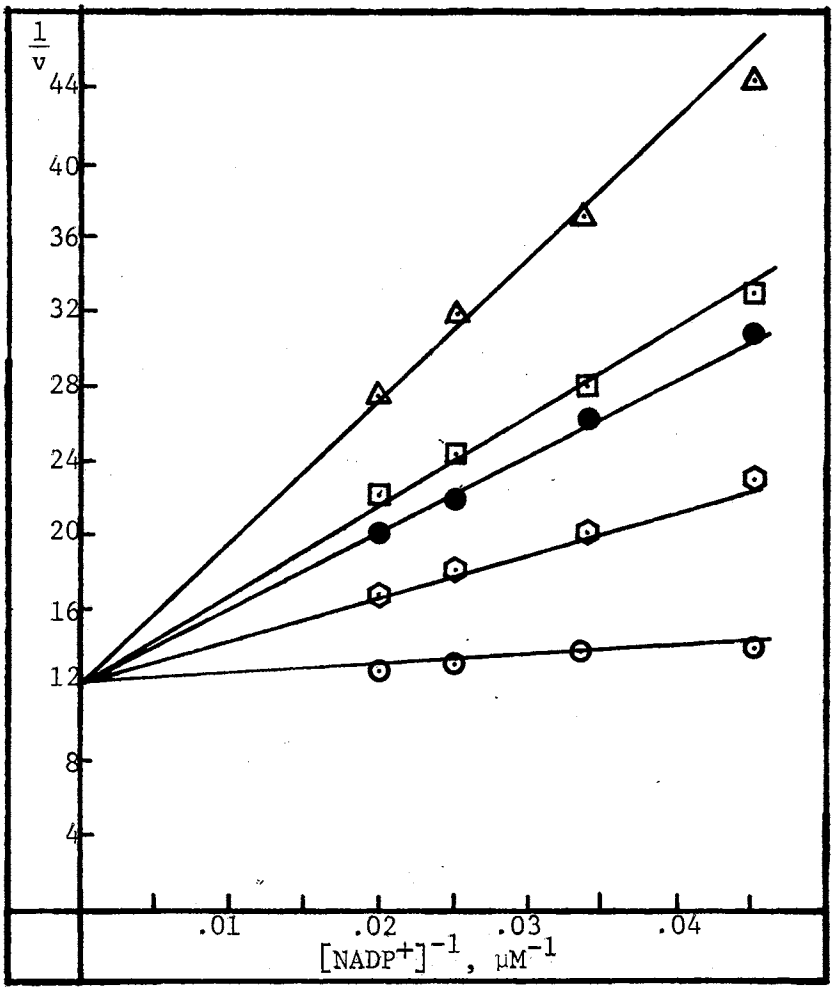

Figure 2. Competitive Inhibition of G6PDH by NADPH. Assay buffer was as listed in Figure 1. NADPH concentrations were 0.0 μM, O-O; 57.5 μM, ⬡-⬡ ; 115 μM, ●-●; 138 μM, □ - □ ; and 230 μM, Δ-Δ.

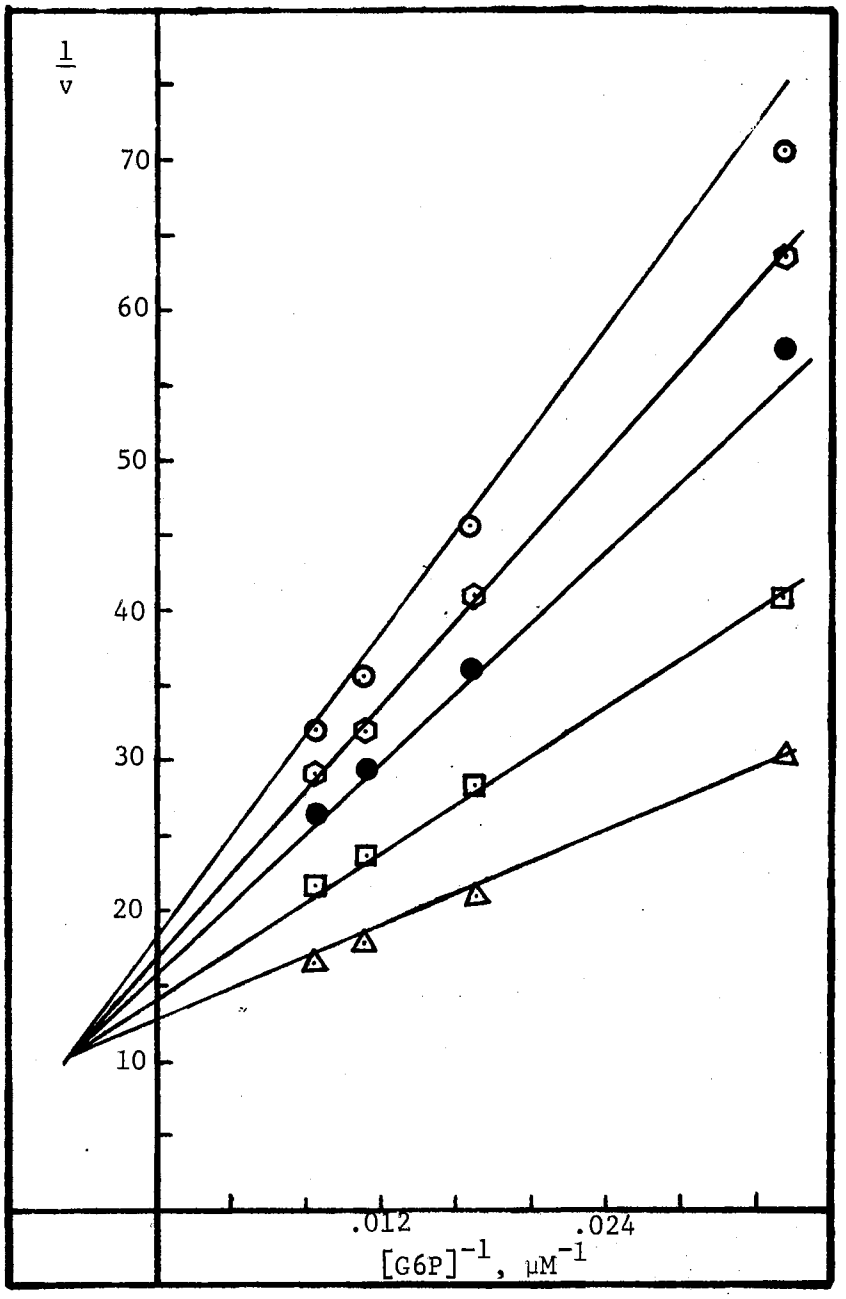

Figure 3. Noncompetitive Inhibition of G6PDN by NADPH. Assay Buffer was the Same as for Figure 1. NADPH Concentrations were 0.0 μM, Δ-Δ; 50.0 μM, □-□ ; 100 μM, ●-●; 150 μM, ⬡-⬡ ; and 200 μM O-O.

substrate analog for G6P in an attempt to form a dead-end complex by the following reaction.

$$\text{E-NADP} + \text{glucosamine 6-P} \rightleftarrows \text{E-NADP-glucosamine 6-P}$$

When studied at glucosamine 6-P and enzyme concentrations which preclude significant contribution to reduction of $NADP^+$ by glucosamine 6-P, such complex formation should exhibit competitive inhibition with respect to G6P. The results of such an experiment are plotted in Figure 4. Where the solid lines are fitted using Equation (2-4). The value of chi-square at the minimum was 29.4 (36 degrees of freedom) indicating a satisfactory description of the data by the model. The best-fit value for K_i was 3.47 ± .06 mM. Competitive inhibition with respect to G6P by glucose, another G6P analog was also obtained in agreement with results by Metzger, et. al. (18).

For an ordered addition of substrates A and B, inhibition by an analog of B (I) forming an enzyme·A·I dead-end complex will be uncompetitive with respect to A as varied substrate. Figure 5 shows the results of an experiment in which the $NADP^+$ concentration was varied at changing, fixed concentrations of glucosamine 6-P with a G6P concentration of 50 μM. Again the solid lines show the results of a fit to Equation (2-4). Using a standard error for $v_{i,measured}$ of 10%, chi-square was 20 (25 degrees of freedom) indicating a satisfactory fit.

As an additional verification of the sequential mechanism of mevalonic kinase Beytia, et al. (29) performed double inhibition experiments using a dead-end inhibitor in addition to product inhibition. A similar experiment was performed on rat liver G6PDH using glucosamine 6-phosphate and NADPH in the presence of subsaturating $NADP^+$ and G6P concen-

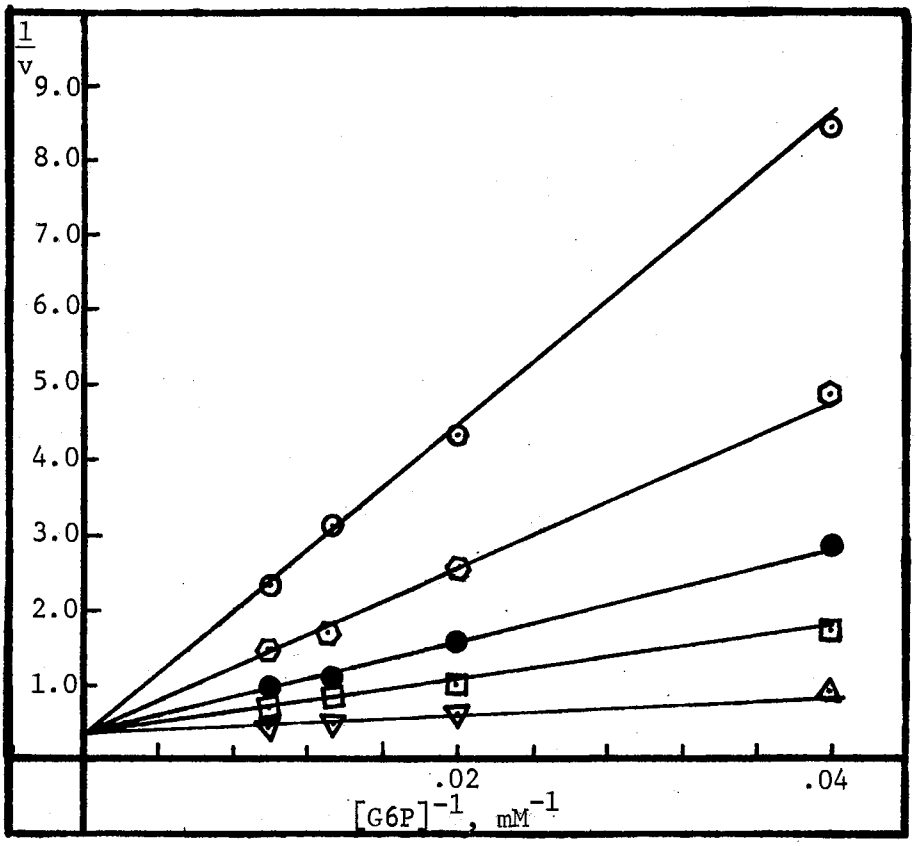

Figure 4. Competitive Inhibition of G6PDH by Glucosamine 6-P. Assay conditions were stated in Figure 1. NADP concentration was 60 μM. Glucosamine 6-P concentrations were 0.0 mM, Δ-Δ; 1.0 mM, □-□ , 2.0 mM, ●-●; 4.0 mM, ⬡-⬡ ; and 8.0 mM, 0-0.

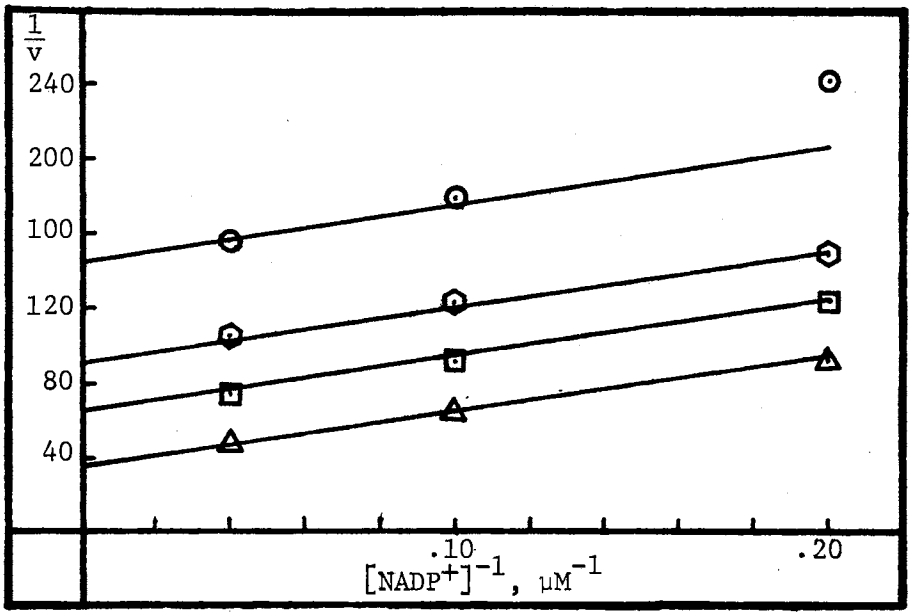

Figure 5. Uncompetitive Inhibition of G6PDH by Glucosamine 6-P. Assay conditions were the same as for Figure 1. The G6P concentration was 100 µM. Glucosamine 6-P concentrations were 0.0 mM, Δ-Δ; 1.0 mM, □-□ ; 2.0 mM ⬡ - ⬡ ; and 4.0 mM O-O.

trations. The data were fitted to Equation (2-5) and the results are shown in Figure 6. The model satisfactorily describes the data as evidenced by the chi-square value at 23.5 (21 degrees of freedom). When the data are plotted as 1/v against product concentration the resultant plot is one of parallel lines as predicted by Equation (2-6) where at constant A and

$$\frac{Vm}{v} = \left(\frac{K_{ia}\,K_b}{K_{iq}\,AB} + \frac{K_a}{A\,K_{iq}}\right) Q + \frac{K_{ia}\,K_b}{AB} + \frac{K_b}{B} + \frac{K_b\,I}{K_i\,B} + \frac{K_a}{A} + 1 \qquad (2\text{-}6)$$

B concentrations, the slope is constant and the inhibitor concentration I enters only into the intercept term.

The kinetic mechanism for erythrocyte G6PDH has been described as a sequential ordered mechanism (12) with coenzyme adding first and being released last from the enzyme. The results effectively rule out a rapid equilibrium random (R.E.R.) mechanism with the formation of a dead-end enzyme-G6P-NADPH complex. This is done by comparing their value for K_b with an independently determined value for the dissociation constant for the second substrate and finding that the two differ by a factor of 17. However, no data concerning the existence of significant levels of a ternary enzyme-G6P-NADP complex was obtained thus not excluding the possibility of a Theorell-Chance mechanism. Initial velocity and product inhibition studies on G6PDH from both L. mesenteroides (13) and C. utilis (11) rule out a rapid equilibrium random plus dead-end inhibition mechanism by the use of NAD^+ as an alternate substrate for $NADP^+$ but again do not rule out a Theorell-Chance mechanism.

Experiments on liver cytoplasmic G6PDH reported here indicate from initial velocity data that the mechanism is sequential, thus excluding

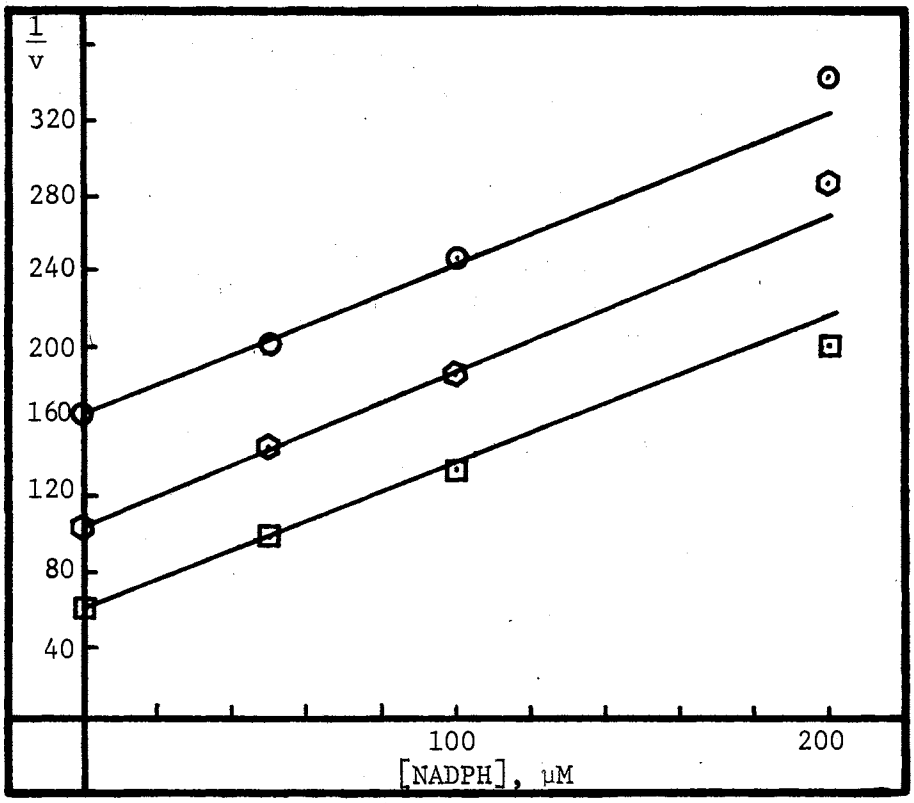

Figure 6. Double Inhibition of G6PDH by NADPH and Glucosamine 6-P. Assay conditions were the same as for Figure 1. The $NADP^+$ concentration was 50 μM and the G6P concentrations were 50 μM. Glucosamine 6-P concentrations were 0.0 mM, □-□ ; 1.0 mM, ⬡-⬡ ; and 2.0 mM, O-O.

ping-pong and random mechanisms. Results from dead-end inhibition studies using G6P analogs are inconsistent with a rapid equilibrium random plus dead-end inhibition mechanism. In such a mechanism, a B substrate analog can be expected to combine with both E and EA enzyme forms. This would result in non-competitive inhibition with respect to substrate A and competitive inhibition with respect to substrate B. The inhibition patterns observed were uncompetitive and competitive with respect to substrates A and B respectively, indicating that the dead-end inhibitor combines with the EA enzyme form alone, consistent with a steady-state ordered mechanism. Exclusion of the Theorell-Chance mechanism might be done by the demonstration of significant central complex concentrations, by dead-end inhibition studies using an inhibitor shown to combine only with central complexes, by product inhibition studies using the first product (6-phosphogluconolactone (6-PGL) in this case), or by isotopic exchange experiments which monitor B-P exchange as B and P are varied in a constant concentration ratio. The latter is the most rigorous test. The instability of 6-phosphogluconolactone clearly complicates efforts to exclude the Theorell-Chance mechanism from consideration.

In summary, results from initial velocity studies, product inhibition, dead-end inhibition, and mixed inhibition kinetics are consistent with an ordered mechanism in which coenzyme adds first and is released last from liver glucose 6-phosphate dehydrogenase. This mechanism is shown in the notation of Cleland (26).

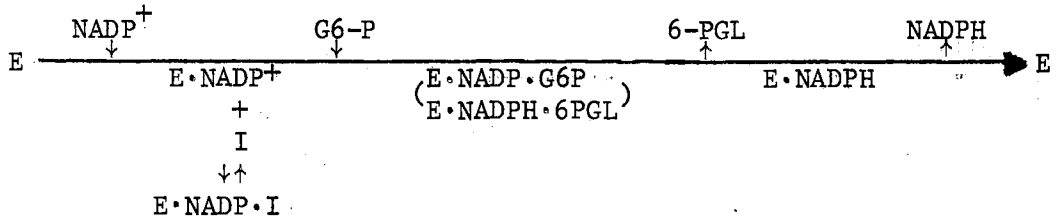

The steady-state mechanism for the rat liver cytoplasmic enzyme is similar to the mechanism for G6PDH from various other sources where $NADP^+$ is the coenzyme.

CHAPTER III

METABOLITE AND CONCENTRATION EFFECTS ON GLUCOSE 6-PHOSPHATE DEHYDROGENASE

Introduction

Numerous studies have been made on the quaternary structure of human erythrocyte G6PDH. Yoshida (10) has done preliminary studies on specific activity as a function of enzyme concentration. This work has shown that the enzyme is fully active (750 U/mg) only at protein concentrations of greater than 0.3 mg/ml. This is a five-fold increase over the specific activity at enzyme concentrations of 7 μg/ml. The physiological implications of this phenomenon are somewhat in question however, due to the rather low cellular enzyme concentration of approximately 6.5 μg/ml and the inability of the mature erythrocyte to respond to environmental changes by increasing protein concentration.

Several observations have indicated that rat liver cytoplasmic G6PDH activity is controlled by a long-term regulation (30). The enzymic activity has been shown to be a function of various dietary states (2). Furthermore, this variation in activity has been demonstrated to be a consequence of enzyme biosynthesis and degradation (31). When these observations are considered in light of evidence that the enzyme quaternary structure is a function of enzyme concentration (4), it becomes reasonable to test the hypothesis that the rat liver cytoplasmic enzyme might behave similar to the erythrocyte enzyme with changes in concentration.

Srere (32) has established a procedure whereby cellular enzyme levels might be estimated from specific activity and homogenate activity data. Using this procedure and published activity data (7,1) the cellular concentration of liver G6PDH is calculated to be approximately 0.2 mg/ml or 30 units/ml in rats fed a high carbohydrate, low fat diet (see Materials and Exp. Proc.) and 0.02 mg/ml (3 Units/ml) in rats subjected to starvation. Clearly then with a 10-fold variation in enzyme activity as a function of diet, the properties of the enzyme as a function of concentration should be investigated.

It has been shown that the mass action ratio for the G6PDH catalyzed reaction in vivo is approximately three orders of magnitude away from the equilibrium constant (1). Krebs (33) has pointed out that among other mechanisms, reaction equilibria may be a controlling force in the regulation of intermediary metabolism. This criterion for metabolic control appears to be in contradiction to an additional criterion proposed by Newsholme and Gevers (34,35) when applied to the G6PDH catalyzed reaction. Namely, the substrate concentration should decrease as the flux through the enzyme catalyzed reaction increases. This clearly does not hold for G6PDH in the various dietary conditions considered by Greenbaum, et al. (1). This apparent contradiction for the substrate glucose 6-phosphate is a result of the relatively minor part played by the hexose monophosphate shunt in G6P utilization. The major control is probably exerted by NADPH. This is a consequence of the high cellular levels of NADPH (3-12 mM) (1) and the rather low value for K_{iq} (10-15 μM). Indeed, denominator terms in the rate equation multiplied by the ratio $[NADPH]/K_{iq}$ will contribute substantially to the sum of all denominator terms. For this reason product inhibition by NADPH is of primary importance in the

short-term regulation of liver cytoplasmic G6PDH (1).

The involvement of additional effectors in the short-term metabolic regulation of liver cytoplasmic G6PDH have been suggested. An ATP inhibition has been reported (36) and contradicted (4). The question of fatty acid inhibition is much more complex.

Since NADPH is utilized in fatty acid biosynthesis, a mechanism of metabolic control by feedback inhibition of G6PDH by either free fatty acids or long chain acyl-coenzyme A derivatives is reasonable. Evidence of inhibition of G6PDH activity by a fat containing diet has been reported (1,4). However, additional studies, in vitro, have shown that the inhibition of rat liver cytoplasmic G6PDH by myristic, lauric, and palmitic acids is prevented by incubation of the enzyme with 10 μM $NADP^+$ prior to the addition of fatty acids (4). The irreversibility of the inhibition suggests that the effect is a result of inactivation. The physiological significance of the inhibition is in question since the cellular level of $NADP^+$ has not been shown to fall below 50 μM (1).

Inhibition of liver cytoplasmic G6PDH by long chain acyl-CoA derivatives has been demonstrated (37,38) with opposing conclusions concerning physiological significance. Taketa and Pogell (38) found that palmityl coenzyme A both inhibited and inactivated crude rat liver glucose 6-phosphate dehydrogenase. These authors found, however, that a wide variety of enzymes, some apparently unrelated to fatty acid metabolism, were activated or inhibited by very low concentrations of the acyl ester. They therefore concluded that the physiological role of acyl-CoA esters in the regulation of intermediary metabolism must be viewed with reservation.

Similar arguments questioning the significance of palmityl-CoA in-

hibition of acetyl-CoA carboxylase have been reported (39). These were answered by the observations that the inhibition did not increase with time of incubation and was reversible and competitive with a potentially physiological activator (citrate) (39).

The question of physiological significance of acyl-CoA inhibition of G6PDH has been discussed with respect to short-term regulation. Evidence for long-term regulation by means of enzyme biosynthesis and degradation includes studies which show the existence of three different G6PDH-inactivating proteins in rat liver cells (21) which act either on $NADP^+$ (a glycohydrolase and a pyrophosphorylase) or on the enzyme itself. This control mechanism is supported also by the previously mentioned $NADP^+$ protection against fatty-acid induced inactivation. In addition, inactivation by a detergent induced disaggregation or by a specific, substrate reversible mechanism could render a protein molecule more susceptible to protease digestion. The latter possibility is supported by studies on glyceraldehyde 3-phosphate dehydrogenase (40) which show a protection by NAD^+ or ATP against chymotrypsin inactivation.

Materials and Experimental Procedures

The enzyme was purified as described earlier. Reaction rate measurements were made as described above for dilute enzyme. Concentrated enzyme measurements were made on a Durrum-Gibson stopped-flow spectrophotometer made by the Durrum Instrument Corporation of Palo Alto, California. In the stopped flow instrument the reactants in separate drive syringes were in a thermostatted water bath. The reaction cell was maintained at the same temperature by circulating water from the water bath through the Kel-F housing surrounding the mixing chamber. Reactant solu-

tions were deairated for 10 minutes by water aspiration before placing them in the instrument. Output from the photomultiplier was monitored by a Tektronix Type 564 storage oscilloscope. Enzyme and $NADP^+$ were stored in one drive syringe and G6P and effectors were stored in the other.

Results and Discussion

Concentrated Enzyme Studies

Results from studies comparing dilute with concentrated enzyme are listed in Table I. The results indicate no significant concentration dependent effects observable upon enzyme specific activity, NADPH product inhibition, ATP inhibition, or dehydroepiandrosterone inhibition. These results are in spite of a previously demonstrated concentration dependent quaternary structure (4) and in marked contrast to those obtained with G6PDH from human erythrocytes (10).

Results from initial velocity and NADPH product inhibition measurements on rat liver cytoplasmic G6PDH in dilute solutions ($\approx 10^{-4}$ mg/ml) are shown in Table II. The results were obtained in the presence of near physiological concentrations of $NADP^+$ (60 μM) and G6-P (200 μM) but at a sub-physiological level of NADPH (200 μM). There is no significant effect by any of the compounds tested upon either enzyme activity or NADPH product inhibition.

Metabolite Effects

Experiments by Yugari and Matsuda (4) have shown that long chain fatty acid inhibition of G6PDH is relieved by $NADP^+$ such that at cellular coenzyme levels there is no inhibition. In addition, they showed

TABLE II

CONCENTRATED ENZYME STUDIES

[G6PDH]	[$NADP^+$]	[G6P]	[NADPH]	[ATP]	[DHEA]	Sp. Act.
6.6×10^{-5} mg/ml	250 µM	400 µM	-------	------	------	129 U/mg
6.6×10^{-5} mg/ml	250 µM	400 µM	-------	2.0 mM	------	120
6.6×10^{-5} mg/ml	250 µM	400 µM	-------	------	100 µM	120
3.3×10^{-1} mg/ml	250 µM	400 µM	-------	------	------	168
3.3×10^{-1} mg/ml	250 µM	400 µM	-------	2.0 mM	------	160
3.3×10^{-1} mg/ml	250 µM	400 µM	-------	------	100 µM	161
1.7×10^{-4} mg/ml	100 µM	200 µM	-------	------	------	150
1.7×10^{-4} mg/ml	100 µM	200 µM	200 µM	------	------	79
2.7×10^{-1} mg/ml	100 µM	200 µM	-------	------	------	141
2.7×10^{-1} mg/ml	100 µM	200 µM	200 µM	------	------	92

that ATP enhanced this inhibition, although incapable of inhibiting the reaction alone. It was therefore decided to investigate the interrelationships among ATP, palmityl CoA and other effectors on the reaction catalyzed by purified G6PDH. These results are shown in Table III. These results indicate that 25 μM palmityl-CoA inhibits slightly but that the inhibition is more than doubled in the presence of 2.0 mM ATP. This inhibition enhancement is not mimiced by 1.0 mM ADP. The presence of 100 μM Acetyl CoA eliminates the palmityl CoA inhibition, has no effect when coupled with ATP, but reduces the palmityl CoA plus ATP inhibition. None of the effectors had any significant effect on the NADPH inhibition. These results are consistent with a model which involves an ATP-dependent change in enzyme conformation, or stabilization of one or several conformations more conducive to palmityl-CoA inhibition. This model is not dissimilar to that proposed for rat liver pyruvate kinase FDP activation (41). The specific effects of Acetyl CoA and ATP argue against non-specific detergent inactivation by palmityl-CoA.

One report (42) has stated that rat liver G6PDH is inhibited 50% by 60 nM palmityl carnitine. In an effort to verify this claim as well as to test effects of additional compounds both on G6PDH activity and on NADPH product inhibition (200 μM NADPH), data were collected on the initial velocities of reactions in the presence of compounds listed in Table V. The results show no significant effects upon either G6PDH activity or NADPH product inhibition. Additional experiments failed to show an effect on G6PDH activity when 2.0 mM ATP was added with palmitoylcarnitine. Differences between these and previously reported results might well be due to different states of enzyme purity.

TABLE III

METABOLITE EFFECTS ON G6PDH ACTIVITY

NADPH	Compound	Concentration	Relative Activity[a]
------	--------	------	100
200 µM	--------	------	50
------	NAD^+	1.0 mM	100
200 µM	NAD^+	1.0 mM	46
------	Ac CoA	100 µM	104
200 µM	Ac CoA	100 µM	51
------	CoA	150 µM	104
200 µM	CoA	150 µM	53
------	ATP	2.0 mM	90
200 µM	ATP	2.0 mM	41
------	GSH	10 mM	98
200 µM	GSH	10 mM	45
------	DHEA	100 µM	98
200 µM	DHEA	100 µM	50
------	PEP	100 µM	95
200 µM	PEP	100 µM	49
------	Citrate	500 µM	93
200 µM	Citrate	500 µM	45
------	NADH	2 µM	98
200 µM	NADH	2 µM	48

[a] Numbers are the averages of from 2-4 determinations corrected to a value of 100 for the uninhibited reaction.

TABLE IV

METABOLITE EFFECTS ON G6PDH ACTIVITY

[NADPH]	[Pal-CoA]	[ATP]	[ADP]	[Ac-CoA]	Relative Activity[a]
-------	-----	------	------	------	100
200 µM	-----	------	------	------	49
-------	25 µM	------	------	------	89
-------	-----	2.0 mM	------	------	100
-------	-----	------	1.0 mM	------	100
200 µM	25 µM	------	------	------	46
200 µM	-----	------	1.0 mM	------	49
-------	25 µM	2.0 mM	------	------	75
-------	25 µM	------	1.0 mM	------	90
200 µM	25 µM	2.0 mM	------	------	41
-------	25 µM	------	------	100 µM	100
-------	-----	2.0 mM	------	100 µM	100
-------	25 µM	2.0 mM	------	100 µM	81

[a]Numbers are the averages of from 2-4 determinations corrected to a value of 100 for the uninhibited reaction.

TABLE V

METABOLITE EFFECTS ON G6PDH ACTIVITY

[NADPH]	Compound	Concentration	Relative Activity[a]
-------	-------------------	-----	100
200 μM	-------------------	-----	49
-------	Malonyl CoA	50 μM	102
200 μM	Malonyl CoA	50 μM	46
-------	6-PGA	80 μM	102
200 μM	6-PGA	80 μM	46
-------	Ac-Carnitine	10 μM	101
200 μM	Ac-Carnitine	10 μM	48
-------	Carnitine	10 μM	102
200 μM	Carnitine	10 μM	45
-------	Palmitoyl Carnitine	10 μM	101
200 μM	Palmitoyl Carnitine	10 μM	48

[a]Numbers are the averages of from 2-4 determinations corrected to a value of 100 for the uninhibited reaction.

CHAPTER IV

CIRCULAR DICHROISM OF GLUCOSE 6-PHOSPHATE DEHYDROGENASE

Introduction

In recent years, circular dichroism (CD) has been used extensively in the estimation of protein secondary structure. Quantitation was originally based upon comparison of protein spectra with spectra of shorter chain synthetic polypeptides, most notably poly-L-lysine (43), at pH extremes consistent with complete random, helical, or pleated sheet conformations. The choice of synthetic polypeptides as standards came under attack first from Saxena and Wetlaufer (44), and later from Yang et al (45,46). This attack was based mostly upon the dissimilarity between random coil of these synthetic peptides at pH extremes and the restricted random coil shown to exist in proteins by X-ray diffraction studies (46). Thus, since the secondary structure could be quantitatively divided into classes for those proteins whose X-ray diffraction studies had been completed, it was decided to use proteins as standards of comparison. This was done first at only one wavelength (44) and later (46) for a range of wavelengths over which secondary structure contributions to circular dichroism were most significant. The most sophisticated of treatments of CD data is by Chen et al. (46). However, the treatment lacks appropriate weighting of the data, inclusion of some constraints, and a means by which to estimate error in the fitted parameters (fraction

of each secondary structure). Therefore a computer program has been written, based upon the standard data previously published (46) which overcomes those deficiencies.

Program Description and Rationale

The model can be described by Equation (4-1).

$$[\theta]_\lambda = f_H[\theta]_{H,\lambda} + f_\beta[\theta]_{\beta,\lambda} + f_R[\theta]_{R,\lambda} \qquad (4\text{-}1)$$

where $[\theta]$ is mean residue molar ellipticity, f_H, f_β, and f_R are fractions α-helix, β-pleated sheet, and remainder, respectively, the latter taken as the sum of all other conformational contributions at wavelength λ. Actually Equation (4-1) is a system of n simultaneous linear equations at n discrete wavelengths. The molar ellipticities $[\theta]_H$, $[\theta]_\beta$, and $[\theta_R]$ of each structural form are calculated at each wavelength by a least squares fit of Equation (4-1) to CD data on five proteins where structure fractions, f_H, f_β and f_R are estimated independently from X-ray diffraction data. Assuming the mean residue ellipticity of each conformation (H, β, and R) is reasonably constant among (and within) all proteins, the structural fractions for other proteins are determined from their CD spectra by application of Equation (4-1) with f's as the adjustable parameters in the least squares minimization.

The FORTRAN program HELIX makes use of two additional physical realities. First, since secondary structure is defined as α-helix, β-pleated sheet (both forms), and all remaining conformations (remainder), Equation (4-2) is necessarily true.

$$f_H + f_\beta + f_R = 1 \qquad (4\text{-}2)$$

Therefore, there are only two parameters rather than three. Second, to have physical meaning, no component fraction can exceed 1 or become negative. Thus Equation (4-1) can be easily transformed into Equation (4-3) with constraints (4-4), (4-5), and (4-6).

$$[\theta]_\lambda = f_H[\theta]_{H,\lambda} + f_\beta[\theta]_{\beta,\lambda} + (1 - f_H - f_\beta)[\theta]_{R,\lambda} \tag{4-3}$$

$$0 \leq f_H \leq 1 \tag{4-4}$$

$$0 \leq f_\beta \leq 1 \tag{4-5}$$

$$0 \leq (1 - f_H - f_\beta) \leq 1 \tag{4-6}$$

However, as f_H and f_β are optimized they are further constrained within the interval [0,1]. That is, if f_H assumes some value greater than 0, then f_β must assume some value less than $1 - f_H$. This constraint is most readily implemented by optimizing the parameters f_H and $f_\beta/(1 - f_H)$ within the intervals [0,1]. For this non-linear regression analysis problem the program STEPIT (23) was selected. Error estimates for f_H and f_β were by the usual linear approximation (24). The weighted sum of squares minimized was the function F, equal to chi-square at the minimum (25).

$$F = \sum_{i=1}^{N} \left\{ \frac{[\theta]_{i,\text{measured}} - [\theta]_{i,\text{fitted}}}{\sigma_i} \right\}^2$$

where N is the number of wavelengths i, $[\theta]_{i,\text{measured}}$ is the mean residue ellipticity measured experimentally, $[\theta]_{i,\text{fitted}}$ is the mean residue ellipticity computed, and σ_i is the standard error in $[\theta]_{i,\text{measured}}$, approximated as 2% of $[\theta]$ at each wavelength. In addition to best fit

values for f_H and f_β, the program computes errors in each, the correlation between them, and the value of F at the minimum. The latter provides an estimate of the quality with which the model describes the experimental data, namely the chi-square criterion for goodness of fit. Initial estimates for f_H are made from data at 222 nm according to a formula published by Chen and Yang (45) and f_β is arbitrarily estimated at 0.5. The program was tested by the use of CD data collected in our laboratory on lactate dehydrogenase, one of the proteins used as a standard by Chen et al. (46). The best-fitted fractions for α-helix and β-pleated sheet were within estimated error of those values published for LDH (46).

Materials and Experimental Procedure

Circular Dichroism (CD) spectra were run on a Cary 61-CD model spectropolarimeter. Samples were in a 1 mm pathlength cylindrical quartz cuvette and the optical path was flushed with nitrogen. The CD instrument had been calibrated with an aqueous solution of d-10-camphor sulfonic acid (Aldrich) using the molar ellipticity value determined by Cassim and Yang (47). Glucose 6-phosphate dehydrogenase had been purified and specific activity determined as previously specified (Chapter II). Spectra were run on G6PDH in the presence of 10^{-4} M $NADP^+$.

Results and Discussion

The fitted values for f_H, f_β, and f_R are shown in Table VI and the fitted curve with experimental points shown in Figure 7. The chi-square value for the fitted curve (12.0) is consistent with the number of degrees of freedom (12) indicating a satisfactory fit of the data to the

model. The results indicate a rather large value for f_H when compaired with the value for LDH (29%) (46). Conformational analysis of yeast G6PDH has been done using ORD (48). The value for Moffitt constant (b_o) obtained, when used in the equation by Chen and Yang (45), predicts 14% α-helix content. In view of the limited data available it is difficult to assess the differences.

TABLE VI

MEAN RESIDUE WEIGHT ELLIPTICITY OF G6PDH

Structure	Best Fit (± Standard Error)
f_H	51.0 ± 1.3
f_β	32.6 ± 5.1
f_R	16.4

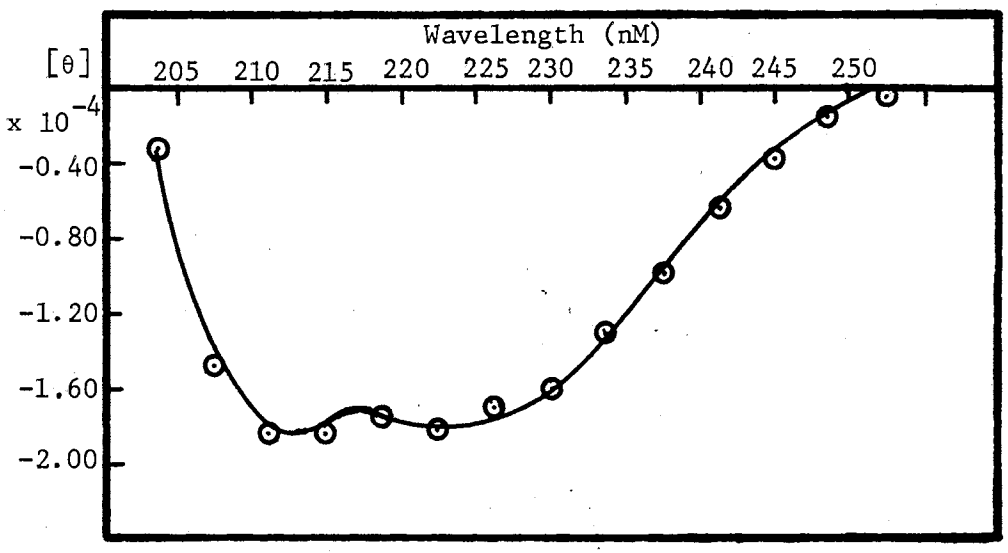

Figure 7. Circular Dichroism Spectrum of G6PDH. Measurements were made at a protein concentration of 50 µg/ml in 20 mM potassium phosphate, pH 7.0 containing 10 µM $NADP^+$.

A SELECTED BIBLIOGRAPHY

(1) Greenbaum, A. L., Gumaa, K. A., and McLean P., (1971), Arch. Biochem. Biophys. 143, 617-663.

(2) Mandula, B., Srivastava, S. K., and Beutler, E., (1970), Arch. Biochem. Biophys. 141, 155-161.

(3) Fitch, W. M. and Chaikoff, I. L., (1960), J. Biol. Chem. 235, 554-557.

(4) Yugari, Y. and Mutsuda, T., (1967), J. Biochem. (Tokyo) 61, 541-549.

(5) Watanabe, A. and Taketa, K., (1972), J. Biochem., 72, 1277-1280.

(6) Holten, D. (1972), Biochim Biophys. Acta 268, 4-12.

(7) Matsuda, T., and Yugari, Y., (1967), J. Biochem., 61, 535-540.

(8) Schmukler, M. (1970) Biochim. Biophys. Acta, 214, 309-317.

(9) Taketa, K. and Watanabe, A. (1971) Biochim. Biophys. Acta, 235, 19-26.

(10) Yashida, A. (1966), J. Biol. Chem. 241, 4966-4976.

(11) Afolayan, A. (1972), Biochemistry 11, 4172-4178.

(12) Soldin, S. J. and Balinsky, D. (1968), Biochemistry 7, 1077-1082.

(13) Olive, C., Geroch, M. E., and Levy, H. R. (1971), J. Biol. Chem. 246, 2047-2057.

(14) Afolayan, A. and Luzzatlo, L. (1971), Biochemistry 10, 415-419.

(15) Luzzatto, L. and Afolayan, A. (1971), Biochemistry 10, 420-423.

(16) Horecker, B. L. and Smyrniotis, P. Z., (1953), Biochim. Biophys. Acta, 12, 98-102.

(17) Bessell, E. M. and Thomas, P., (1973), Biochem. J. 131, 83-89.

(18) Metzger, R. P., Metzger, S. A., and Parsons, R. L., (1972), Arch. Biochem. Biophys., 149, 102-109.

(19) Geisler, R. W., McClure, A. M., and Housen, R. J. (1973) Biochim. Biophys. Acta., 327, 1-10.

(20) Watanabe, A. and Taketa, K. (1973), Arch. Biochem. Biophys., 158, 43-52.

(21) Bonsignore, A., DeFlora, A., Mangiavolti, M. A., Lorenzoni, I., and Alemà, S. (1968), Biochem. J. 106, 147-154.

(22) Lowry, O. H., Rosebrough, N. J., Farr, A. L., and Randall, R. J. (1951) J. Biol. Chem., 193, 265-275.

(23) Chandler, J. P. (1971) STEPIT, Quantum Chemistry Program Exchange, Indiana University Chemistry Department, Program 66.

(24) Bevington, P. R. (1969) Data Reduction and Error Analysis for the Physical Sciences, McGraw-Hill Book Company, New York.

(25) Hamilton, W. C. (1969) Statistics in the Physical Sciences, Ronald Press Company, New York.

(26) Cleland, W. W. (1963), Biochim. Biophys. Acta., 67, 104-137.

(27) Cleland, W. W. (1963), Biochim. Biophys. Acta., 67, 173-187.

(28) Fromm, H. J., (1964), Biochim. Biophys. Acta., 81, 413-417.

(29) Beytia, E., Dorsey, J. K., Marr, J., Cleland, W. W., and Porter, J. W. (1970), J. Biol. Chem., 245, 5450-5458.

(30) Bonsignore, A. and DeFlora, A. (1973), in Current Topics in Cellular Regulation (Horecker, B. L. and Stadtman, E. R., ed.) Vol. 6, pp. 21-62, Academic Press, New York.

(31) Tepperman, H. M., and Tepperman, J., (1963) in Advan. Enzyme Regul. (Weber, G. ed.) Vol. 1, pp. 121-136.

(32) Srere, P. A. (1967) Science, 158, 936-937.

(33) Krebs, H. A. (1969) in Current Topics in Cellular Regulation (Horecker, B. L. and Stadtman, E. R., eds.) Vol. 1, p. 49, Academic Press, New York.

(34) Newsholme, E. A., and Gevers, W., (1967) in Vitamins and Hormones (Harris, R. S., Wool, I. G. and Loraine, J. A. eds) Vol. 25, pp. 1-87, Academic Press, New York.

(35) Rolleston, F. S. (1973) in Current Topics in Cellular Regulation (Horecker, B. L. and Stadtman, E. R., eds) Vol. 6, p. 54, Academic Press, New York.

(36) Avigad, G., (1966), Proc. Nat. Acad. Sci. U.S., 56, 1543-1547.

(37) Eger-Neufeldt, I., Teinzer, A., Weiss, L., and Wieland, O. (1965) Biochim. Biophys. Res. Comm. 19, 43-48.

(38) Taketa, K. and Pogell, B. M. (1966), J. Biol. Chem. 241, 720-726.

(39) Volpe, J. J. and Vagelos, P. R. (1973), in Am. Rev. Biochem. Vol. 42, p. 30.

(40) Shin, B. C. and Carraway, K. L. (1973), J. Biol. Chem. 248, 1436-1444.

(41) Spivey, H. O., Flory, W., Peczon, B. D., Chandler, J. P., and Koeppe, R. E. (1974) Biochem. J. (in press).

(42) Marquis, N. R., Francesconi, R. P., and Villee, C. A. (1968) in Adv. Enz. Reg. (Pergamon Press, New York), Vol. 6, p. 47.

(43) Greenfield, N. and Fasman, G. D. (1969), Biochemistry, 8, 4108-4116.

(44) Saxena, U. P. and Wetlaufer, D. B. (1971), Proc. Nat. Acad. Sci. U.S.A. 68, 969-972.

(45) Chen, Y-H, and Yang, J. T. (1971) Biochem. Biophys. Res. Comm. 44, 1285-1291.

(46) Chen, Y-H, Yang, J. T., and Martinez, H. M. (1972), Biochemistry 11, 4120-4131.

(47) Cassim, J. Y. and Yang, J. T. (1969), Biochemistry, 8, 1947-1951.

(48) Jirgensons, B. (1966), Die Makromal. Chem. 91, 74-86.

PART TWO

IMPROVEMENTS IN NUMERICAL METHODS FOR ANALYZING PROTON AND METAL-LIGAND EQUILIBRIUM CONSTANTS, AND APPLICATION TO THE MAGNESIUM: 5-PHOSPHORIBOSYL-1-PYROPHOSPHATE SYSTEM

CHAPTER V

INTRODUCTION

It is often necessary to know the acid dissociation constants and metal ligand stability constants for the weak acids and bases frequently encountered in chemistry and biology. These charged ligands often bind one or more metal ions to any of several protonated and unprotonated species. The determination of these equilibrium constants has for the most part been based on the method of competitive complex formation utilizing titration data in which pH is measured in a solution of known total metal and ligand concentrations as acid or base is added.

Techniques for the analysis of such data range in sophistication from graphical methods for limiting cases to the more general computerized methods which treat a variety of models (for a discussion of these various methods, see references 1a, 1b). All of the common methods rely on the use of a mole balance equation each for ligand and metal plus an electrical neutrality equation:

$$[L]_T = [L] + \sum_{\ell=1}^{L_{max}} \sum_{m=0}^{M_{max}} \sum_{n=0}^{H_{max}} [L]^{\ell}[M]^{m}[H^+]^{n}\beta_{\ell mn} \qquad (5\text{-}1)$$

$$[M]_T = [M] + \sum_{\ell=0}^{L_{max}} \sum_{m=1}^{M_{max}} \sum_{n=0}^{H_{max}} [L]^{\ell}[M]^{m}[H^+]^{n}\beta_{\ell mn} \qquad (5\text{-}2)$$

$$[H^+] + Z_M[M] + Z_L[L] = [OH^-] + [\text{Titrant}]_{\text{Acid}} - [\text{Titrant}]_{\text{Base}} + [X]_{MX} + \sum_{\ell=0}^{L_{max}} \sum_{m=0}^{M_{max}} \sum_{n=0}^{H_{max}} [L]^{\ell}[M]^{m}[H^+]^{n}\beta_{\ell mn} \qquad (5\text{-}3)$$

where $[L]_T$ and $[M]_T$ are the total concentrations of ligand and metal respectively, $[L]$ and $[M]$ are the concentrations of uncomplexed ligand and metal respectively, L_{max}, M_{max}, and H_{max} are the maximum values allowed for ℓ, m, and n respectively, and

$$\beta_{\ell mn} = [M_m L_\ell H_n][H^+]^n/[L]^\ell[M]^m \ . \qquad (5\text{-}4)$$

The general case in which ℓ, m, and n can assume integer values greater than one has been most efficiently treated by Tobias and Yasuda (2) with subsequent modification of the method by Perrin and Sayce (3). The Tobias-Yasuda method minimizes the sum of squares of the residual function R where:

$$R = C_H - \sum_{\ell}\sum_{m}\sum_{n} n[L]^\ell[M]^m[H^+]^n \beta_{\ell mn} - [H^+] + [OH^-] \ .$$

where C_H is defined by the concentration difference between the total dissociable protons of the initial complex and the net of added base titrant. Although these residuals are weighted by the inverse of experimental variances of R at each data point, a deficiency remains in that the $[M]$ and $[L]$ used unnecessarily contain error propagated from the experimental pH measurements.

In an effort to overcome the shortcomings of the existing techniques and taking advantage of the fact that the complexes encountered most frequently in biochemical and often in chemical problems are mono-nuclear species, we have sought to develop an algorithm capable of determining metal-ligand stability constants for this special case. For this case ℓ in Equations (5-1), (5-2), and (5-3) is equal to one. The integers m and n may assume larger values depending upon the extent of proton dissociation and complexation. This gives three equations, which are linear

in [L] and are (usually) higher order polynomials in [M] and [H^+]. Our TITER algorithm is a package of stable, modern methods not subject to divergence or oscillation which are used for the solution of the numerical problems arising at each level of the calculations. The method is designed to adjust the parameters (K_{ai},K_i) on the basis of a comparison of an experimentally determined dependent variable (pH) with a fitted value for that dependent variable, the final computed value of which is independent of the experimental value. As a result, the favorable statistical properties deriving from the classical method of least-squares are obtained.

As an example of the special case in which one ligand molecule forms a stable complex with one or more metal ions we have chosen the magnesium pyrophosphate system:

$$\begin{array}{ccccccc} H_3L^- & \overset{K_{a1}}{\rightleftarrows} & H_2L^{2-} & \overset{K_{a2}}{\rightleftarrows} & HL^{3-} & \overset{K_{a3}}{\rightleftarrows} & L^{4-} \\ & & & & \downarrow\uparrow K_1 & & \downarrow\uparrow K_2 \\ & & & & MHL^- & \rightleftarrows & ML^{2-} \\ & & & & & & \downarrow\uparrow K_3 \\ & & & & & & M_2L \end{array}$$

in which L is pyrophosphate, M is magnesium, K_{ai} are acid dissociation constants, and K_i are metal-ligand stability constants. In our procedure the equilibrium constants are treated individually rather than as overall or cumulative formation constants or stability products (β_n) as was done by Tobias and Yasuda.

CHAPTER VI

PROGRAM DESCRIPTION AND RATIONALE

The problem may be conveniently divided into three computational levels. [The innermost level derives from the nature of Equations (5-1), (5-2), and (5-3).] Since Equations (5-1), (5-2) and (5-3) are each linear in [L] for the special case considered here, this variable may be eliminated by substituting the expression for [L] from Equation (5-3) into each of the other two equations. The result is two new Equations P1 and P2, polynomials in [M] and $[H^+]$. For a given $[H^+]$, experimentally established $[L]_T$ and $[M]_T$, and guesses for K_{ia} and K_i, a positive, real root [M] each for Equations P1 and P2 may be computed. This is the inner level of the computation. The difference between these roots depends upon the selected value for $[H^+]$, and yet to maintain internal consistency the two values for [M] must be equal. It remains then to find the value of $[H^+]$ for which the equality is satisfied. This is the middle computational level which consists of finding a real zero for the scaled function $\phi([H^+])$:

$$\phi([H^+]) = \frac{[M]_{P1} - [M]_{P2}}{[M]_{P1} + [M]_{P2}} \qquad (6\text{-}5)$$

where $[M]_{P1}$ and $[M]_{P2}$ are the positive real roots of the polynomials P1 and P2 respectively. The value of pH at the zero of the function is then taken as the fitted value of the dependent variable for each data

point. A pegasus modified regula falsi method (PEGAS) is used.

Least-squares theory then calls for systematic adjustment of the parameters (K_{ai},K_i) such that the weighted sum of squares of the residuals, in this case $F(K_{ai},K_i)$ (Equation (6-6) is minimized:

$$\chi^2 = \sum_{i=1}^{N} \left(\frac{pH_{i,measured} - pH_{i,fitted}}{\sigma_i}\right)^2 \qquad (6\text{-}6)$$

where N is the number of data points and σ_i is the standard deviation of the measured pH at data point i. This outer computational level utilizes either of two descent methods for non-linear least-squares minimization. The first, STEPIT, (4) is a direct search method and the second, MARQ, is Marquardt's method which combines the favorables properties of the Gauss-Newton method and the method of steepest descent. Initial guesses for the parameters are based on previously determined values for similar constants in analogous compounds. Fitting to the logs of the parameters rather than to the parameters themselves allows STEPIT to move the parameter values into a region close to the minimum quite rapidly even though the initial guesses may be several orders of magnitude different from the best-fit values. From this point in parameter space the rapidly converging Marquardt's method completes the minimization process with many fewer chi-square evaluations than most direct search methods.

The middle computational level is potentially slow since a real zero of the function $\phi([H^+])$ must be found for each data point every time $F(K_{ia},K_i)$ is evaluated. Therefore, the measured pH values at each data point are used as starting points for the calculations in the first evaluation of $F(K_{ia},K_i)$. In subsequent $F(K_{ia},K_i)$ evaluations, however, each solution of $\phi([H^+])$ is begun from the best previous set of solu-

tions. Thus, as the minimization advances each zero finding iteration begins from better initial guesses. At each step, however, the root is computed to high precision and is independent of the experimental value.

The search for a real zero of $\phi([H^+])$ also requires that the roots of polynomials P1 and P2 be evaluated several times at each data point. The accuracy of the initial guesses from which the polynomial root-finding process iterates determines the time spent in each iteration. For the first $F(K_{ia},K_i)$ evaluation the total metal concentration is used as the starting point in determining $[M]_{P1}$ at the first data point. The root of that polynomial is the initial guess for the root of P2 at the first data point. The final value of [M] at the zero of $\phi([H^+])$ for the first data point is taken as the initial guess for the root of P1 at the second data point and the process is continued throughout the data set for the first chi-square evaluation. For subsequent $F(K_{ia},K_i)$ evaluations the stored values for [M] at each data point associated with the best previous fit initialize each root finding process as in the search for the real zero of $\phi([H^+])$ above. This optimization of the middle and inner computational levels considerably shortens otherwise time consuming operations.

Extremely poor parameter estimates as well as grossly inappropriate models occasionally produce a $\phi([H^+])$ function which has no real zeroes. When that problem arises $\phi^2([H^+])$ is minimized and a large number added to chi-square, thus encouraging the outer level minimizer to withdraw from the region of parameter space producing the problem. Similarly, polynomials P1 and P2 which either have no real roots or have roots which lie outside of the region $0 \leq [M] \leq [M]_T$, result in chi-square being increased, additively, by an amount proportional to the deviation

outside the constrained region. The program thus contains internal criteria for physical reality.

When, in the absence of metal, one wishes to determine the K_{ai}, the appropriate mole balance equation for ligand and the electrical neutrality relation are expressed as functions in [L]. Elimination of this quantity between the two functions and the determination of the largest, positive real root of the resulting polynomial in $[H^+]$ provides a value for $pH_{i,fit}$ to be used as above in the determination of chi-square. This results in a much shorter computation.

Whether acid dissociation or metal-ligand stability constants are to be determined there is the necessity of multiplying polynomials and collecting terms into the desired coefficients. As models increase in complexity this process becomes tedious and assumes a high probability of error. The program therefore contains a subroutine which numerically evaluates the product of two polynomials and collects terms into an array of coefficients which can then be submitted to a polynomial root finder.

Finally, it is frequently desirable to obtain computed values for the concentrations of each of the species included in the model at each data point pH. In addition, the value of the formation function $\bar{n}$ (Equation (6-7)) at each data point is often informative.

$$\bar{n} = \frac{[L]_T - [L]}{[M]_T} \qquad (6\text{-}7)$$

Solution of Equation (5-1), (5-2), or (5-3) for [L] using the best fit parameters and fitted values for $[H^+]$ and [M] and subsequent substitution of the appropriate quantities into Equations (5-4) and (6-7) readily

lead to the desired concentrations and values for $\bar{n}$. This computation is optional, but when the appropriate print switch is turned on, these values are printed out with corresponding fitted pH values.

CHAPTER VII

PYROPHOSPHORIC ACID

Materials and Methods

Reagents were analytical grade. The NaOH was carbonate free and had been standardized by titration to a phenol red endpoint with standard HCl (constant boiling) which was also used as the acid in the potentiometric titrations. Standard pH buffers were obtained from Thomas (pH 7.00 ±.02), Curtin (pH 4.01 ± .01) and Fisher (pH 10.00 ± .02) laboratory supply houses.

Potentiometric Titrations

Titrations of pyrophosphate were made with Radiometer (Copenhagen) instruments including: PHM 25/TTT11 titrater, PHA 925a scale expander graduated in 0.01 pH unit, TTA31 titration assembly, SBU1 syringe gurette, G2222C glass electrode, and K4112 calomel electrode. Titrations were performed at room temperature (27^{o}) on 7.5 ml of approximately 3 mM pyrophosphate in KCl solution, which was magnetically stirred. Argon, saturated with water by passage through a gas scrubber bottle, was bubbled through the titration solutions. KCl was added to solutions to give 180 mM in nominal ionic strength, μ', calculated as

$$\mu' = 3[MgCl_2]_t + [KCl]_t$$

where brackets and subscripts indicate total concentrations.

Subsequent calculations of concentrations of all ionic species from best fit constants revealed that the total ionic strength was within the range of 0.193 to 0.224 M for all titrations. The titrant was 0.100 N HCl and a maximum of 1 ml titrant was added from a 2.5 ml syringe in each titration. The SBU1 micrometer and syringe (Hamilton no. 1002) were calibrated to within 0.2% precision by weights of water delivered to weighing bottles. Values of pH and micrometer readings were recorded manually at approximately 0.2 pH unit intervals following each increment of titrant. Each titration was completed within 20 to 30 min. Tests on electrode reproducibility and drift against buffers at pH 4.00, 5.00, 6.01, and 7.00 indicated that combined systematic and random errors were within 0.03 pH unit.

Results

Table VII shows the results of curve fitting to pH titration data collected on approximately 3 mM sodium pyrophosphate. There are 45 data points encompassing the range of pH 4 to pH 9 with and without 3 mM $MgCl_2$. Fit I is the result of fitting to a seven parameter model (six equilibrium constants and the total pyrophosphate concentration). The fitted value for log K_{a1} has the greatest error. This is due primarily to the fact that the titration data is only through pH 4 thus precluding $H_3P_2O_7^-$ from attaining a concentration sufficient to determine K_{a1} accurately. Fixing this constant at a previously reported value (determined in higher ionic strength) such that it is not adjusted during the minimization (Fit II) results in a somewhat larger chi-square indicating a less satisfactory fit. The elimination of $H_3P_2O_7^-$ from the model (Fit

TABLE VII

ASSOCIATION CONSTANTS FOR SODIUM PYROPHOSPHATE

Parameter	Fit I	Corrected Error	Fit II	Fit III	Literature*	Error
pK_{a1}	3.09	0.113	(2.52)[a]	-----	2.52[b]	0.06
pK_{a2}	6.14	0.019	5.97	5.95	6.08[b]	0.06
pK_{a3}	8.37	0.013	8.22	8.21	8.45[b]	0.06
Log K_1	3.12	0.032	3.09	3.06	3.06[c]	0.06
Log K_2	5.08	0.024	5.07	5.05	5.41[c]	0.06
Log K_3	-30	∞	0.38	-6.27	7.75[c]	0.09
$[P_2O_7]$	3.21 mM	0.02	3.24	3.18	-----	
χ^2	51		60	74	-----	
D.F.	38		39	39		

[a]Value held constant during fit.

[b]Ref. 12 determined 0.1 M ionic strength (Swarzonbach & Zurc (1950) Montach 81, 202).

[c]Ref. 13 determined at 1 M ionic strength.

*Literature values are overall stability const, β's; not stepwise, K's (this does not change any value except K_3).

III) results in a further increase in chi-square. The values for the errors in each parameter are corrected to give a chi-square probability of 0.5. The corresponding corrected errors in pH data are .034 pH unit.

Table VIII lists the ranges of calculated concentrations for the various species throughout the two titrations. The uncomplexed ligand concentration was calculated at each data point using the fitted values for pH and magnesium ion concentration in the ligand conservation or metal conservation equation. Additional species concentrations were calculated from Equation (5-4).

Figure 8 shows the fitted titration curves for pyrophosphate in the presence and absence of 3.0 mM magnesium chloride. The pH is plotted as a function of titrant concentration corrected for volume increase. The points were experimentally determined and the curves were fitted.

Table IX is the lower triangle of the correlation matrix for the fitted parameters as determined from Fit I (Table VII). All correlations are low enough to prevent "ill-conditioning" associated with the optimization of very highly correlated parameters, although the association constants for the most highly protonated species are highly correlated with the total ligand concentration.

Discussion

Figure 8 illustrates the ability of the alogorithm to fit a seven parameter pyrophosphate model to the data. The logs of six equilibrium constants were fitted simultaneously with the log of the total ligand concentration. Fit I (Table VII) was based on data collected in 0.18 M ionic strength at 27°C. The value for K_{a1} is poorly determined but the best-fit K_{a2} agrees well with the literature value. The best-fit K_{a3}

TABLE VIII

PYROPHOSPHATE SPECIES CONCENTRATIONS

Species	Concentration Range (Molarity)	
	No. Magnesium	3 mM Magnesium
$P_2O_7^{4-}$	$1.20 \times 10^{-8} - 2.73 \times 10^{-3}$	$5.41 \times 10^{-9} - 1.71 \times 10^{-4}$
$HP_2O_7^{3-}$	$7.65 \times 10^{-5} - 2.69 \times 10^{-3}$	$4.98 \times 10^{-5} - 7.66 \times 10^{-4}$
$H_2P_2O_7^{2-}$	$4.65 \times 10^{-7} - 2.86 \times 10^{-3}$	$1.10 \times 10^{-6} - 2.68 \times 10^{-3}$
$H_3P_2O_7^{-}$	$3.72 \times 10^{-13} - 8.56 \times 10^{-5}$	$5.41 \times 10^{-12} - 1.16 \times 10^{-4}$
$MgHP_2O_7^{-}$		$1.71 \times 10^{-6} - 2.82 \times 10^{-3}$
$MgP_2O_7^{2-}$		$3.25 \times 10^{-5} - 1.12 \times 10^{-3}$
$Mg_2P_2O_7$		$\sim 10^{-42}$

TABLE IX

LOWER TRIANGLE OF THE CORRELATION MATRIX FOR PYROPHOSPHATE MODEL PARAMETERS

Log K_{a1}	1.00						
Log K_{a2}	0.67	1.00					
Log K_{a3}	0.37	0.25	1.00				
Log K_1	0.42	0.58	0.10	1.00			
Log K_2	0.21	0.36	0.54	0.60	1.00		
Log K_3	0.0	0.0	0.0	0.0	0.0	1.00	
$\text{Log}[P_2O_7]_T$	-0.91	-0.81	-0.39	-0.39	-0.20	0.0	1.00
	Log K_{a1}	Log K_{a2}	Log K_{a3}	Log K_1	Log K_2	Log K_3	Log $[P_2O_7]_T$

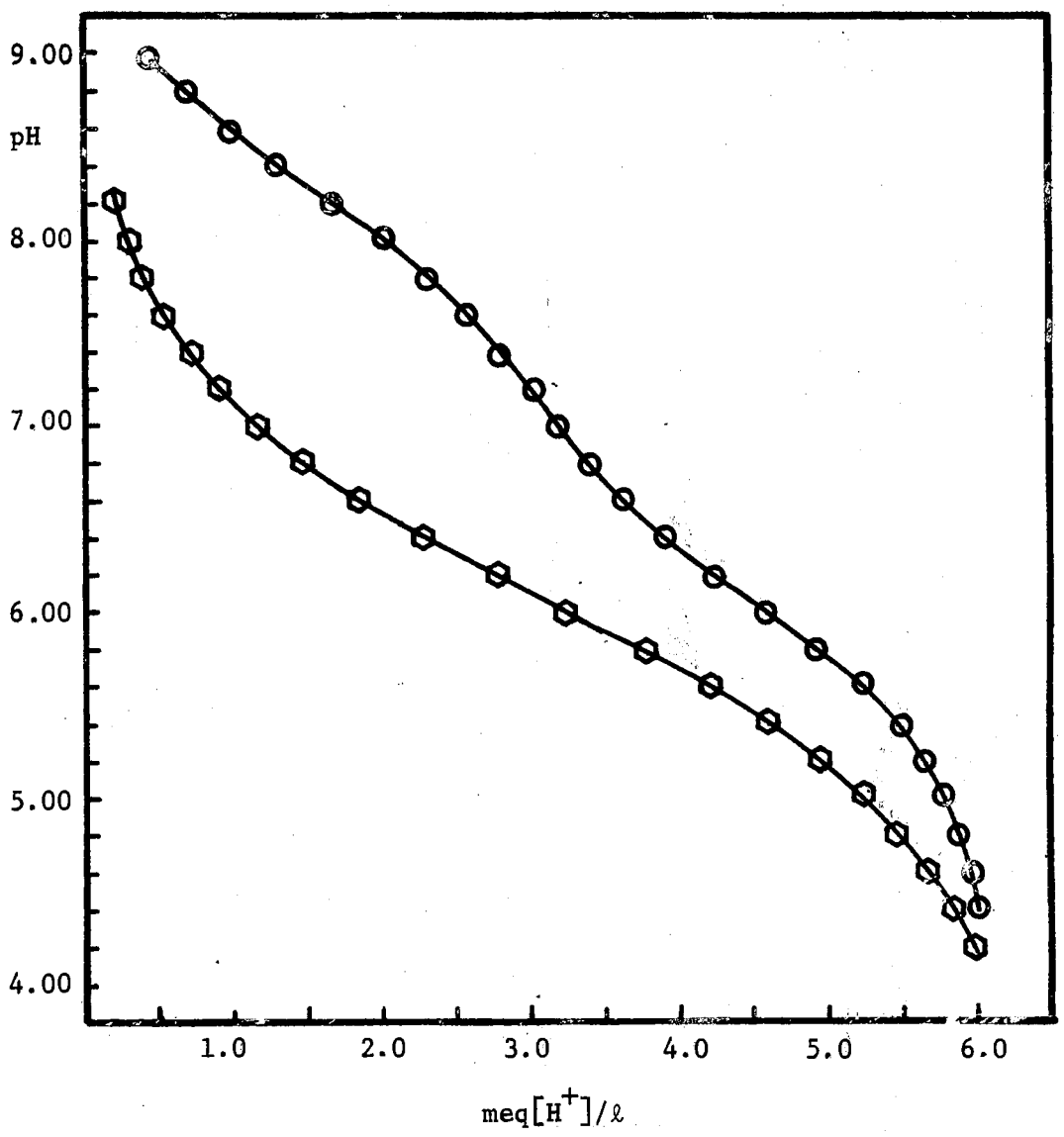

Figure 8. Potentiometric Titration of Pyrophosphate. Titration was by hydrochloric acid in the presence of 0.0 mM $MgCl_2$, O-O; and 3.0 mM $MgCl_2$, O - O .

deviates more from the previously determined value than experimental error would predict. This is due to the ionic strength difference, more evident in the association constants for more highly charged species.

The response of the program to an association constant describing a complex containing two magnesium ions per ligand molecule (K_3) demonstrates the inability of the experimental conditions ($[Mg]_T < [L]_T$) to allow appreciable formation of that complex. This situation is demonstrated by an attempt by the least squares minimizer to push the parameter value into a region of parameter space in which the parameter no longer affects the fit. This is the result of a situation similar to that depicted in Figure 9. Large values for the association constant are incompatible with the data and this is reflected in large values for chi-square. The minimizer finds that chi-square is decreased as the parameter value is decreased until M_2L attains a negligible concentration. At that point a further decrease will not improve chi-square.

The most definitive criterion for the effect of a parameter on the fit is the error estimate. Errors in the fitted value for a parameter are estimated by the usual linear approximation (5). This is effected by measuring the response of chi-square to small alterations in each parameter about its fitted value. For the situation depicted in Figure 9 the estimated error is infinite as was obtained in Fit I of Table VII for pK_3.

The quality of the pyrophosphate fit as judged by the chi-square "goodness-of-fit" criterion is highly dependent upon the total ligand concentration; that is, one or more equivalence points of the titration curve are accurately determined, as expected. This is evidenced by the relatively small error estimated for the fitted concentration which is

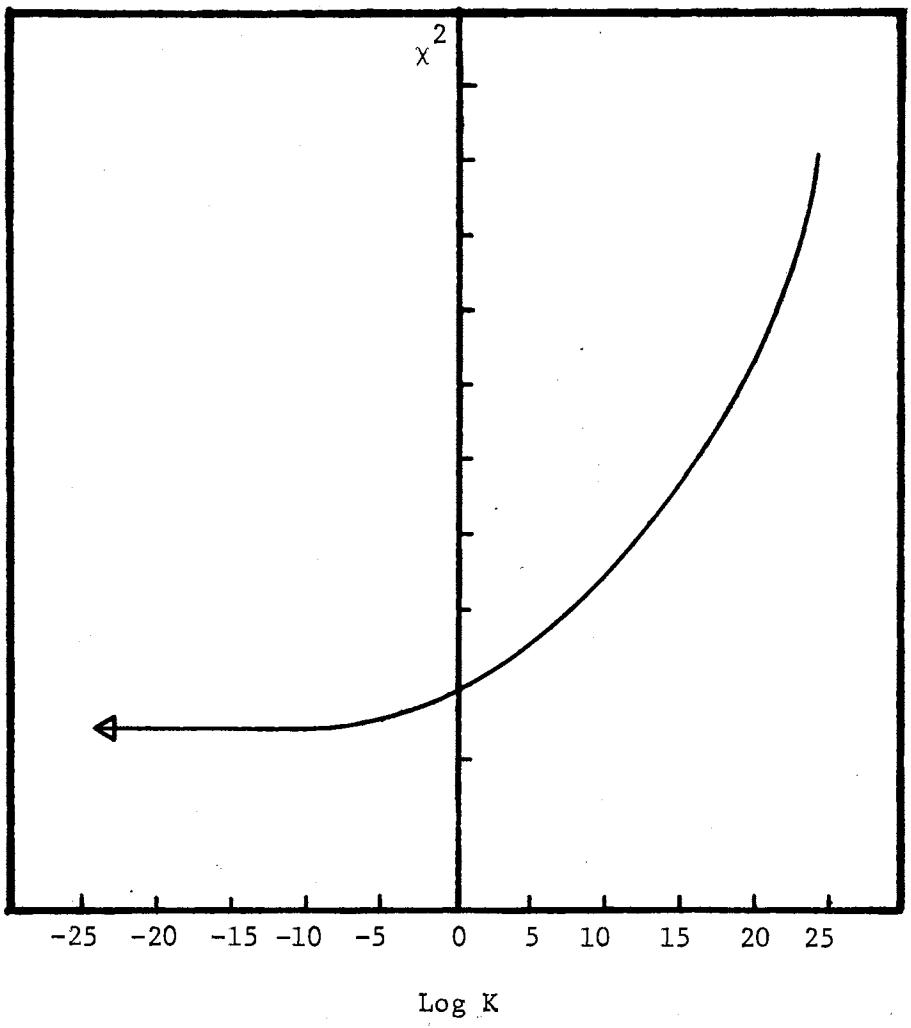

Figure 9. Chi-square as a Function of Log K. See text for details.

consistent with a rapid increase in chi-square as the concentration is varied about its fitted value.

The computer program TITER is advantageous over the most sophisticated of its predecessors, (2) and (3), both in design and numerical execution in several respects. First, it utilizes a root-finder instead of "simple iteration" in the determination of [M] thus taking advantage of the relative speed of the former over the latter. In addition, most simple iterative techniques are capable of stable oscillation or divergence whereas our root finding precludes such behavior. Secondly, TITER utilizes either of two descent methods for the non-linear least-squares refinement of parameters. These methods are much less likely to move the parameters into a distant and physically meaningless region of parameter space, and in the event this does occur, either method has the means of returning to more reasonable values of the parameters whereas a pure Gauss-Newton technique does not have this ability. In addition, neither descent method in TITER has shown the difficulties encountered with highly correlated parameters described by Tobias and Yasuda. Highly correlated parameters, it might be added, are necessarily a consequence of a model in which several equilibrium constants are associated with a single species. Thirdly, procedures in which two implicit calculations of a function such as $\bar{n}$, in which neither is based solely upon experimentally determined values, and which seek to minimize the square of the difference (2) are inherently inferior to those which compare, as by chi-square, experimentally determined and calculated quantities.

CHAPTER VIII

DETERMINATION OF PHOSPHORIBOSYL PYROPHOSPHATE-MAGNESIUM ACID DISSOCIATION AND STABILITY CONSTANTS

The importance of 5-phosphoribosyl-1-pyrophosphate (PRPP) in the direct formation of purine and pyrimidine nucleotides from free bases was first established by Kornberg et al. in 1955 (6). This was followed by several studies demonstrating the function of PRPP in the biosynthetic pathways of tryptophan (7), histidine (8), and nicotinamide coenzymes (9,10). In many of the enzyme catalyzed reactions which involve PRPP, magnesium ions are required for activity. Among these are phosphoribosyltransferase reactions (11-13), and those catalyzed by adenylate pyrophosphorylase (14), and phosphoribosyl pyrophosphate synthetase (15). This has been interpreted as a requirement by the enzymes for a magnesium bound form of PRPP rather than the free ligand, analogous to the Mg-ATP requiring kinases. Quantitative evidence for this interpretation has been lacking due to the unavailability of values for the magnesium - PRPP stability constants.

Previous attempts at estimating the physiologically important magnesium - PRPP stability constants proved difficult due primarily to the instability of PRPP and the presence of impurities (9). Subsequent kinetic studies on enzymes utilizing PRPP as a substrate used crude estimates for the stability constants (6,7) or saturated the system with Mg^{2+}.

Therefore the present study was undertaken to provide more accurate estimates for the magnesium - PRPP association constants at an ionic strength of 0.2 M. The equilibrium constants were determined from pH titration data on PRPP in the presence and absence of Mg^{2+}.

Materials and Methods

Materials

The tetra-sodium salt of PRPP, the barium salt of ribrose-5-P and the mixed enzymes, orotidine 5'-P pyrophosphorylase and orotidine 5'-P decarboxylase from yeast were purchased from the Sigma Chemical Company, St. Louis, Mo. All other chemicals were of reagent grade. Heavy metal contaminants were extracted from magnesium chloride with dithizone (16) and Mg^{2+} concentration subsequently determined by standard NaOH titration of the eluate from a Dowex 50-H^{+} resin onto which an aliquot of the stock $MgCl_2$ solution had been placed. The NaOH was carbonate free and had been standardized by titration to a phenol red endpoint with standard HCl (J. T. Baker DILUT-IT) which was also used as the acid in the potentiometric titrations. Standard pH buffers were obtained from Thomas (pH 7.0 ± .02) Curtin (pH 4.01 ± .01) and Fisher (pH 10.00 ± .02) laboratory supply companies.

PRPP Purification and Analysis

PRPP was purified by the technique of Khorana, et al. (17) except that the pooled PRPP sample eluted from the column was concentrated by lyophilization instead of rotary evaporation, and the sample was increased to 100 mg for chromotography on a 2.2 x 4.2 cm column of Dowex 1-2X, Cl^{-}. Between preparations the column was regenerated by passing four

bed volumes of 1 M LiCl over the resin followed by 10 bed volumes of glass distilled water. The resultant PRPP was stored in a vacuum desiccator over phosphorous pentoxide at -20°C. The preparation was found to maintain stability within assay reproducibility for at least two months. Commercial analysis showed a 1:1 carbon to lithium ratio.

PRPP was assayed enzymatically by the method of Kornberg et al. (18) on a Coleman 124 spectrophotometer equipped with a Coleman #0319 thermostatted cell holder, #801 scale expander, and a #165 recorder. Assay concentrations were 0.3 mM orotate, 2.0 mM magnesium chloride, 5.86 mg/ml PRPP, and 0.3 units per ml orotidine 5'-phosphate pyrophosphorylase and orotidine 5'-phosphate decarboxylase (mixed enzymes) in a 1 cm pathlength cuvette. The reference cell contained 0.3 mM orotate. All reagents were prepared in 20 mM Tris hydrochloride buffer, pH 8.0.

Thin Layer Chromatography was carried out on precoated microcrystalline cellulose plates (5 cm x 20 cm x 250 μ, Type Q2, Quantum Industries) at room temperature. The chromatograms were developed with 7:3 (v/v) Ethanol:1.0 M Ammonium Acetate, pH 7.5, as suggested in the P-L Biochemicals Catalog. The chromatograms were sprayed with fresh Hayne's reagent (19) heated for ten minutes at 100°C, and sprayed with 1M stanuous chloride. R_f values of ribose-5-Phosphate standards and PRPP were 0.27 and 0.03 respectively. A minimum detectible ribose-5-P was 3 μg of the barium salt. A barely detectible amount of ribose-5-P was found in 41 μg of PRPP. The maximum amount of impurity consistent with this and the enzymatic analysis is 7.5 mole %.

Data analysis was done using the TITER algorithm developed in our laboratories. This program minimizes the function F by adjusting the equilibrium constants in the calculated pH_{fit} function.

$$F = \sum_{i=1}^{N} \left(\frac{pH_{i,fit} - pH_{i,exp.}}{\sigma_i} \right)^2 \qquad (8\text{-}1)$$

where N is the number of data points and σ_i is the estimated standard deviation in the $pH_{exp.}$, initially estimated to be 0.03 pH units. Titrations of 180 mM KCl with standard acid required negligible acid compared with the PRPP titrations. Omission of this blank from the titration had no affect on the fit.

An ionic strength, μ, near 0.2M was used to correspond to ionic strengths *in vivo* and thus analytical concentrations are used throughout. Concentrations of H^+ and OH^- ($[H^+]$ and $[OH^-]$) were calculated from data and Equations (2) and (3) in Bates (20) and Harned and Owen (21) respectively, giving

$$-\log[H^+] = pH + \log \gamma_H = pH - 0.14 \qquad (8\text{-}2)$$

$$-\log[OH^-] = \log K'_W + \log[H^+] = 13.75 + \log[H^+] \qquad (8\text{-}3)$$

where γ stands for activity coefficient and $K'_W = \frac{a_{H_2O}}{\gamma_H \gamma_{OH}} K_W$, with K_W equal to the thermodynamic dissociation constant of water (21). The variation of total μ from 0.193 to 0.224 M affects the values of $-\log[H^+]$ and $-\log[OH^-]$ by less than 0.01, and thus an average $\mu = 0.21M$ is quoted for the measurements.

Results and Discussion

Previous studies on the stability of PRPP in solution (18) have demonstrated rapid destruction at low pH or elevated temperatures. In order

to assess the extent of decomposition during the titration we incubated 3 mM PRPP in 180 mM KCl at pH4 and pH7 and in 3 mM $MgCl_2$ at pH4 and pH7. Aliquots were removed and PRPP assayed enzymatically as a function of time. No detectable decomposition occurred in any of the incubation solutions for 90 minutes.

For titrations of the pentalithium salt of PRPP in the presence of Mg^{2+}, the following model was considered:

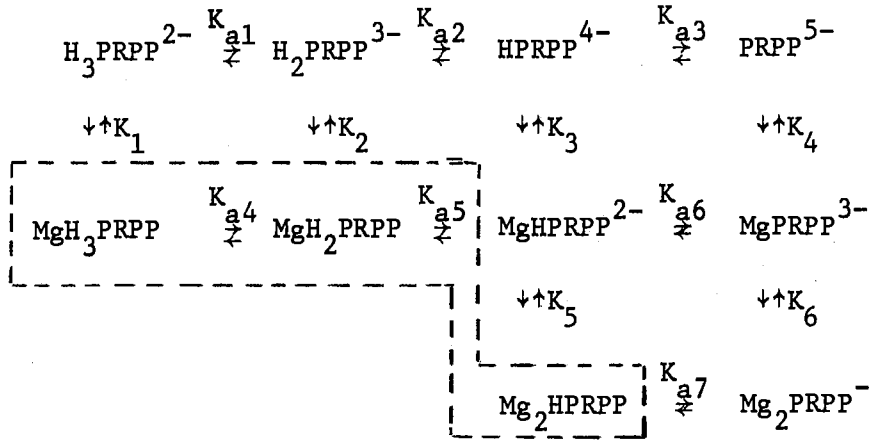

where K_{ai} are the acid dissociation constants and K_i are the Mg^{2+} - PRPP stability constants.

From the behavior of K_{a4}, K_{a5} and K_{a7} early in the minimization it was concluded that none of the species enclosed in the dashed line of the above model attained significant concentrations above pH4. These constants were therefore fixed at initial estimates until convergence of the other seven parameters (six equilibrium constants plus the total PRPP concentration) was achieved as summarized in Table X. Starting with these values, a second convergence was obtained with all ten independent constants free, but none of the parameters were changed significantly in this second fit. The resultant fit was satisfactory by the chi-square criterion for goodness of fit (22).

TABLE X

PRPP EQUILIBRIUM CONSTANTS AND CONCENTRATION

Parameter	Fitted Values[a]	Errors[b]	Origin[c]
pK_{a1}	2.81	0.05	1-PP
pK_{a2}	5.99	0.01	2-P
pK_{a3}	6.84	0.01	2-PP
pK_{a4}	(-1.00)[d]		
pK_{a5}	(2.00)[d]		
pK_{a6}	6.32	0.02	2-P
pK_{a7}	(-2.79)[c]		
Log K_4	3.18	0.03	PP
Log K_6	1.55	0.03	P
Log K_3	(2.70)[e]		PP
$[PRPP]_t$	3.84 mM	0.01 mM	

[a]Molar equilibrium constants.

[b]Standard deviations giving chi-square equal to number degrees of freedom.

[c]Suggested origin of dissociating proton or Mg^{2+}: P = orthophosphate, PP = pyrophosphate; 1- and 2- = primary and secondary hydroxyl groups, respectively.

[d]Values in parentheses were held constant; see text.

[e]Calculated from log K_3 = log $(K_4 K_{a3}/K_{a6})$.

Errors in each parameter were estimated by the usual linear approximation (5, 22) and corrected to give a chi-square (equal to the function F at the minimum) equal to the number of degrees of freedom ($\nu = 38$). Standard deviations in pH calculated by this criterion were ±0.02 in good agreement with initial estimates (±0.03).

Table XI shows the correlation matrix among those parameters actively involved in the minimization process. In no instance is a correlation large enough to arrest the minimization process ("ill-conditioning"). Equilibrium constants which are most highly correlated are those associated with $MgPRPP^{3-}$, the only species participating significantly in three simultaneous equilibria. Species concentrations in Table XII were calculated from fitted equilibrium constants. It is evident that MgH_3PRPP, MgH_2PRPP^-, and Mg_2HPRPP concentrations are insiginficant within the pH and Mg^{2+} concentration ranges of the experiment. This is in agreement with results reported for the analogous triphosphate-magnesium system (23). The species H_3PRPP^{2-} attains a barely significant concentration and thus K_{a1} is less accurately determined than any of the other fitted equilibrium constants and its correlation with total PRPP concentration is high.

The best fit value for the total PRPP concentration is considerably higher than that estimated by enzymatic assay (3 mM). The fitted concentration of PRPP of 3.84 mM gives an effective molecular weight for the pentalithium salt of 472 g/mole implying 89% purity when compared with the anhydrous molecular weight and in close agreement with the 92.5% purity evidenced by thin layer chromatography. This is in contrast to an effective molecular weight of 609 g/mole given by enzymatic assay. The concentration calculated from the titration data is considered much

TABLE XI

LOWER TRIANGLE OF THE CORRELATION MATRIX
FOR THE PRPP MODEL PARAMETERS

pK_{a1}	1.00						
pK_{a2}	0.63	1.00					
pK_{a3}	-0.12	-0.31	1.00				
pK_{a6}	0.12	0.10	-0.41	1.00			
log K_4	0.13	0.27	0.52	-0.79	1.00		
log K_6	-0.04	0.02	-0.36	0.91	-0.80	1.00	
$\log[PRPP]_t$	-0.90	-0.79	0.17	-0.11	-0.16	-0.03	1.00
	pK_{a1}	pK_{a2}	pK_{a3}	pK_{a4}	log K_4	log K_6	$\log[PRPP]_t$

TABLE XII

PRPP SPECIES CONCENTRATIONS (mM)

Species	0.0 mM Mg^{2+}	3.0 mM Mg^{2+}	60.0 mM Mg^{2+}
$PRPP^{5-}$	7.97×10^{-5} - 3.50	9.47×10^{-5} - 1.22	1.62×10^{-4} - 1.28×10^{-2}
$HPRPP^{4-}$	4.69×10^{-2} - 2.16	5.07×10^{-2} - 1.26	2.35×10^{-2} - 1.00×10^{-1}
H_2PRPP^{3-}	3.74×10^{-3} - 3.43	2.56×10^{-2} - 3.36	5.34×10^{-3} - 2.20
H_3PRPP^{2-}	1.84×10^{-3} - 7.05×10^{-2}	5.60×10^{-7} - 9.56×10^{-2}	5.22×10^{-7} - 4.00×10^{-2}
$MgPRPP^{3-}$		4.43×10^{-4} - 1.82	1.44×10^{-2} - 1.18
$MgHPRPP^{2-}$		6.19×10^{-2} - 8.20×10^{-1}	5.68×10^{-1} - 2.45
MgH_2PRPP^{-}		1.23×10^{-11} - 5.08×10^{-9}	1.60×10^{-10} - 6.79×10^{-8}
MgH_3PRPP		2.69×10^{-16} - 1.45×10^{-10}	1.22×10^{-9} - 1.56×10^{-14}
Mg_2PRPP^{-}		3.84×10^{-5} - 5.01×10^{-2}	2.53×10^{-2} - 2.03
Mg_2HPRPP		6.15×10^{-12} - 5.20×10^{-11}	1.11×10^{-9} - 4.85×10^{-9}

more accurate than that determined by enzymatic assay as indicated by the small calculated error in PRPP concentration (Table X), a consequence of the large variation in the function F in Equation (8-1) with changes in PRPP concentration. The enzymatic assay for PRPP is especially insensitive due to the small absorbance change of the reaction (~ 0.19) in the presence of large overall absorbance (~ 1.3) due principally to orotate. Smaller amounts of orotate did not appear to give complete reactions and we suspect this is also true to a significant extent with the higher orotate concentrations used in our assays.

Attempts to characterize the effects of contaminant upon the fitted constants by numerical methods were two-fold. Fitting to a model containing pyrophosphate, ribose-5-phosphate, and PRPP using literature values for contaminate stability constants but allowing percent decomposition to be fitted resulted in variable results depending upon initial parameter guesses. The complex model necessitated very time consuming function evaluations and encountered "local minima". Error free data generated from a contaminant model failed to produce satisfactory fits, in spite of gross alterations in parameter values, with a variety of minimization routines. These results are likely due to the inherently high correlations among parameters describing such complex models.

Assignments of the constants to functional groups are suggested in Table X. All constants appear normal when compared to analogous compounds (23) with these assignments, suggesting that the 1- and 5-phosphate groups have little effect on each other's binding constants. The largest difference noted as the lower metal stability constant of $MgPRPP^{3-}$ (log K = 3.2) than Mg/ADP (log K = 3.6). This is probably the result of the competitive binding of K^{+} ions to PRPP.

The consequences of alkali metal ions, M^+, binding competitively with $[H^+]$ and $[Mg^{2+}]$ to the ligand are simple to predict in principle. The apparent magnesium-ligand stability constant ignoring this competition, as above is given by

$$K^a_{Mg^{2+}} = \frac{[MgL^{3-}]}{[Mg^{2+}]([L^{5-}] + [ML^{4-}])} \qquad (8\text{-}4)$$

while the stoichiometric stability constant corrected for alkali metal ion binding is (25)

$$K_{Mg^{2+}} = \frac{[MgL^{3-}]}{[Mg^{2+}][L^{5-}]} = K^a_{Mg^{2+}} (1 + K_{M^+}[M^+]) \qquad (8\text{-}5)$$

at present, however, the magnitudes of the alkali metal ion binding constant, K_{M^+}, are in doubt. From direct electrode measurements, Mohar and Rechnitz et al. (26) calculate thermodynamic stability constants, K_{M^+}, for ADP and ATP, which are nearly 50 times the stoichiometric stability constants previously calculated by Smith and Alberty (27) from pH titration data at 0.2 ionic strength. Some of this discrepancy is a result of the lower activity coefficients at 0.2 ionic strength. But Rechnitz believes that the majority of the difference is error resulting from the erroneous assumption in the Smith and Alberty method that tetra-n-propylammonium cation does not bind to ADP or ATP.

Further study, and probably additional data, are needed to answer the questions raised by Mohan and Rechnitz and we plan to continue our investigations of these questions. At present, however, we would emphasize that the apparent constants reported in this thesis should be accurate for calculating the quantity of Mg^{2+} bound to PRPP in an electrolyte

solution similar in composition to physiological fluids, as were the solutions used in these determinations. Since Na^+ and K^+ have very similar binding affinities for the phosphates, Mg^{2+} binding constants should be little affected by substitutions between Na^+ and K^+ at constant ionic strength. In fact we believe that until accurate estimates of activity coefficients of free (unbound) polyphosphates are known at 0.2 ionic strength, the apparent stability constants in the presence of Na^+ or K^+ are more pertinent to some biochemical studies than either the thermodynamic constants or the constants determined in the presence of tetraalkylammonium salts. In the latter case, difficulties arise not only due to uncertainties about binding of the alkyl-ammonium ions to phosphates, but also due to the potentially large changes in solvent activities caused by the hydrophobic alkyl groups at these high concentrations (28).

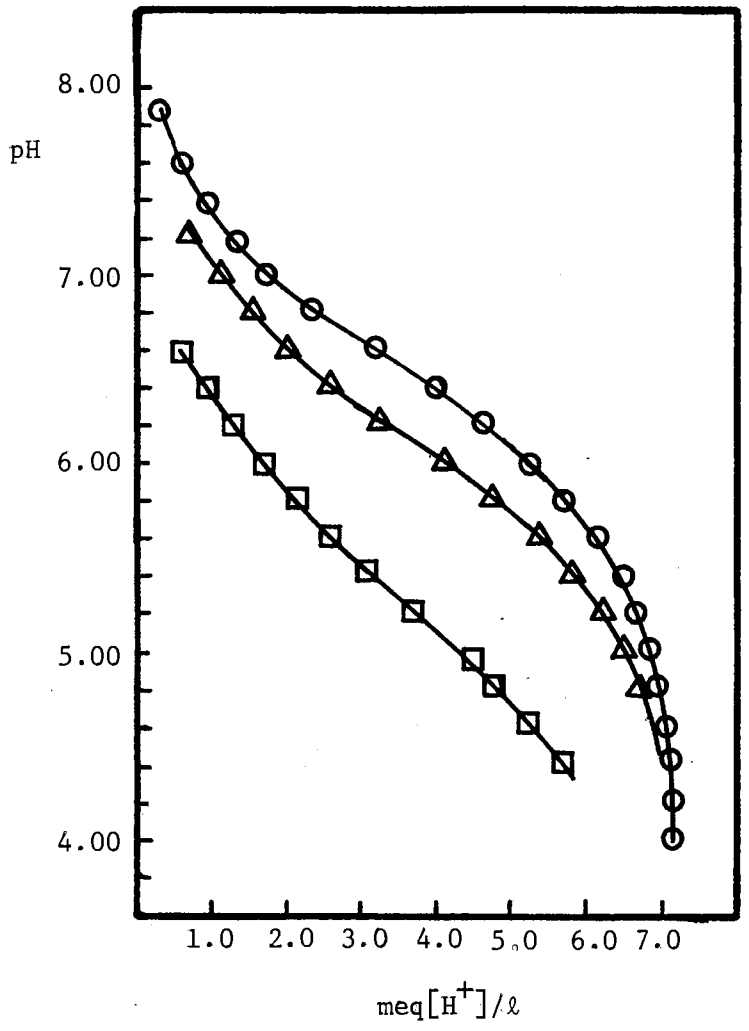

Figure 10. Potentiometric Titration of PRPP. The titrant was hydrochloric acid in the presence of 0.0 mM $MgCl_2$, O-O; 3.0 mM $MgCl_2$, Δ-Δ; and 60.0 mM $MgCl_2$, □-□.

A SELECTED BIBLIOGRAPHY

(1) a. Rossotti, F. J. C. and Rossotti, H. (1961) The Determination of Stability Constants and Other Equilibrium Constants in Solution, McGraw-Hill Book Company, New York.
b. Rossotti, F. J. C., Rossotti, H. S., and Whewell, R. J. (1971) J. Inorg. Nucl. Chem., 33, 2051-2065.

(2) Tobias, R. S. and Yasuda, M. (1963) Inorganic Chemistry 2, 1307-1310.

(3) Perrin, D. D. and Sayre, I. G. (1967) J. Chem. Soc. (A) 82-89.

(4) Chandler, J. P. (1971) STEPIT, Quantum Chemistry Program Exchange, Indiana University Chemistry Department, Program 66.

(5) Bevington, P. R. (1969) Data Reduction and Error Analysis for the Physical Sciences, McGraw-Hill Book Company, New York.

(6) Kornberg, A., Lieberman, I., and Simms, E. S. (1955) J. Biol. Chem. 215, 389-402.

(7) Yanofsky, C. (1956) J. Biol. Chem. 223, 171-184.

(8) Moyed, H. S. and Magasanik, B. (1957) J. Am. Chem. Soc. 79, 4812-4813.

(9) Preiss, J. and Handler, P. (1958) J. Biol. Chem. 233, 488-492.

(10) Preiss, J. and Handler, P. (1958) J. Biol. Chem. 233, 443-500.

(11) Krenitsky, T. A., Neil, S. M., Elion, G. B., and Hitchings, G. H. (1969) J. Biol. Chem. 244, 4779-4784.

(12) Krenitsky, T. A., Papaioannon, R., and Elion, G. B. (1969) J. Biol. Chem. 244, 1263-1270.

(13) Holmes, E. W., McDonald, J. A., McCord, J. M., Wyngaarden, J. B., and Kelley, W. N. (1973) J. Biol. Chem. 248, 144-150.

(14) Berlin, R. D. (1969) Arch. Bioch. Biophys. 134, 120-129.

(15) Switzer, R. L. (1971) J. Biol. Chem. 246, 2447-2458.

(16) Morrison, J. F. and Uhr, M. L. (1966) Biochim. Biophys. Acta 122, 57-74.

(17) Khorana, H. G., Fernandes, J. F., and Kornberg, A. (1958) J. Biol. Chem. 230, 941-948.

(18) Kornberg, A. (1961) in Biochemical Preparations (Meister, A. ed.) Vol. 8, p. 113, John Wiley and Sons, Inc., New York.

(19) Stahl, E. (1969), Thin Layer Chromatography, 2nd ed. pp. 886-887, Academic Press, Inc., New York.

(20) Bates, R. G. (1964) Determination of pH, p. 92, John Wiley, New York.

(21) Harned, H. S. and Owen, B. B. (1958) The Physical Chemistry of Electrolyte Solutions, 3rd Edition, p. 635 and p. 752, Reinhold, New York.

(22) Hamilton, W. C. (1969) Statistics in the Physical Sciences, Ronald Press Company, New York.

(23) Lambert, S. M. and Walters, J. I. (1957) J. Am. Chem. Soc. 79, 4262-4265.

(24) Lambert, S. M. and Walters, J. I. (1957) J. Am. Chem. Soc. 79, 5606-5608.

(25) Johnson, M. J. (1960) The Enzymes, 3, 408-417.

(26) Mohan, M. S. and Rechnitz, G. A. (1972) J. Am. Chem. Soc., 92, 5839-5842.

(27) Smith, R. M. and Alberty, R. A. (1956) J. Am. Chem. Soc., 60, 180-183.

(28) Frank, H. S. and Wen, W.-Y. (1957) Disc. Far. Soc., No. 27, 133-140.

VITA

Richard Edward Thompson

Candidate for the Degree of

Doctor of Philosophy

Thesis: I. PROPERTIES OF RAT LIVER CYTOPLASMIC GLUCOSE 6-PHOSPHATE DEHYDROGENASE
II. IMPROVEMENTS IN NUMERICAL METHODS FOR ANALYZING PROTON AND METAL-LIGAND EQUILIBRIUM CONSTANTS, AND APPLICATION TO THE MAGNESIUM: 5-PHOSPHORIBOSYL-1-PYROPHOSPHATE SYSTEM

Major Field: Biochemistry

Biographical:

Personal Data: Born in Wichita, Kansas, October 17, 1946, the son of Richard C. and Joan E. Thompson.

Educational: Graduated from Wichita High School Southeast, Wichita, Kansas in 1964; received the Bachelor of Science degree in Chemistry from Wichita State University, Wichita, Kansas in 1968; received the Master of Science degree in Chemistry from Wichita State University, Wichita, Kansas in 1969; completed requirements for the Doctor of Philosophy degree on May 11, 1974.

Professional Experience: Served as graduate teaching assistant at Wichita State University 1968-1969; employed as chemist at St. Francis Hospital 1968-1970; employed as Instructor at Wichita State University Department of Chemistry 1969-1970; served as graduate research assistant at Oklahoma State University Department of Biochemistry 1970-1974.

Professional Organizations: Member of the American Chemical Society, member of the Society of Sigma Xi.